GEORGIA INSTITUTE OF TECHNOLOGY — OFFICE OF CONTRACT ADMINISTRATION

PROJECT ADMINISTRATION DATA SHEET

[x] ORIGINAL [ ] REVISION NO. _____

Project No. E-20-640 DATE 2/1/82

Project Director: Dr. Achintya Haldar School/~~Lab~~ Civil Eng.

Sponsor: National Science Foundation

Type Agreement: Grant No. CEE-8111691

Award Period: From 1/1/82 To 9/30/83* (Performance) 9/30/83 (Reports)

Sponsor Amount: $31,699 Contracted through:

Cost Sharing: $ 1,609 (E-20-327) GTRI/~~GTEX~~

Title: Probabilistic Evaluation of Damage Potential in Earthquake - Induced Liquefaction in a 3-D Soil Deposit

ADMINISTRATIVE DATA OCA Contact Faith G. Costello

1) Sponsor Technical Contact: Program Officer

William W. Hakala
Earthquake Hazards Mitigation Section
Division of Civil & Environ. Eng.
Directorate for Engineering
NSF
Washington, DC 20550
(202) 357-9500

2) Sponsor Admin/Contractual Matters:

Lois A. Shapiro
AAEO/ENG Branch, Sec. I
Division of Grants & Contracts
Directorate for Administration
NSF
Washington, DC 20550
(202) 357-9626

Defense Priority Rating: N/A Security Classification: N/A

RESTRICTIONS

See Attached NSF Supplemental Information Sheet for Additional Requirements.

Travel: Foreign travel must have prior approval – Contact OCA in each case. Domestic travel requires sponsor approval where total will exceed greater of $500 or 125% of approved proposal budget category.

Equipment: Title vests with GIT

COMMENTS:

*Includes a 6 month unfunded flexibility period. No charges may be incurred after this date.

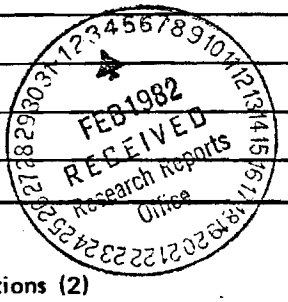

COPIES TO:

Administrative Coordinator
Research Property Management
Accounting
Procurement/EES Supply Services
Research Security Services
~~Reports Coordinator (OCA)~~
Legal Services (OCA)
Library
EES Public Relations (2)
Computer Input
Project File
Other _____

FORM OCA 4/81

EORGIA INSTITUTE OF TECHNOLOGY OFFICE OF CONTRACT ADMINISTRATION

SPONSORED PROJECT TERMINATION/CLOSEOUT SHEET

Date 12/7/83

oject No. E-20-640 School/~~Lab~~ Civil Engr.

cludes Subproject No.(s)

oject Director(s) Dr. Achintya Haldar GTRI / ~~GIT~~

onsor National Science Foundation

tle Probabilistic Evaluation of Damage Potential in Earthquake - Induced Liquefaction in a 3-D Soil Deposit

fective Completion Date: 9/30/83 (Performance) 12/30/83 (Reports)

rant/Contract Closeout Actions Remaining:

- [ ] None
- [X] Final Invoice or Final Fiscal Report
- [ ] Closing Documents
- [X] Final Report of Inventions If Positive
- [ ] Govt. Property Inventory & Related Certificate
- [ ] Classified Material Certificate
- [ ] Other

ontinues Project No. Continued by Project No.

OPIES TO:

oject Director
esearch Administrative Network
esearch Property Management
ccounting
ocurement/EES Supply Services
~~esearch Security Services~~
eports Coordinator (OCA)
gal Services
Library
GTRI
Research Communications (2)
Project File
Other

rm OCA 60:1028

SCEGIT–83–117

PROBABILISTIC EVALUATION OF DAMAGE POTENTIAL IN EARTHQUAKE–INDUCED LIQUEFACTION IN A 3–D SOIL DEPOSIT

By

Achintya Haldar

Technical Report of Research

Supported by

THE NATIONAL SCIENCE FOUNDATION

Grant No. CEE-8111691

November 1983

GEORGIA INSTITUTE OF TECHNOLOGY
A UNIT OF THE UNIVERSITY SYSTEM OF GEORGIA
SCHOOL OF CIVIL ENGINEERING
ATLANTA, GEORGIA 30332

NATIONAL SCIENCE FOUNDATION
Washington, D.C. 20550

FINAL PROJECT REPORT
NSF FORM 98A

PLEASE READ INSTRUCTIONS ON REVERSE BEFORE COMPLETING

PART I–PROJECT IDENTIFICATION INFORMATION

1. Institution and Address	2. NSF Program	3. NSF Award Number
Georgia Institute of Technology School of Civil Engineering Atlanta, Georgia 30332	Earthquake Hazard Mitigation Program	CEE-8111691
	4. Award Period From 1.1.82 To 9.30.83	5. Cumulative Award Amount $31,699

6. Project Title
Probabilistic Evaluation of Damage Potential in Earthquake-Induced Liquefaction in a 3-D Soil Deposit

PART II–SUMMARY OF COMPLETED PROJECT *(FOR PUBLIC USE)*

A three-dimensional probabilistic liquefaction model is developed to estimate the risk of damage due to earthquake-induced liquefaction. The model considers the uncertainty in the seismic loading and all the major site-related geotechnical parameters in a liquefaction problem. The scale of fluctuation of a parameter is important input information representing the three-dimensional statistical characteristics of the deposit. Several methods available to calculate the scale of fluctuation are discussed. Some practical alternatives for geotechnical applications are proposed. Damage is defined in terms of differential settlement and rotation in this study. To estimate the allowable values of these parameters, all major codes, standards, and guidelines are reviewed and compared. The deficiencies and non-uniformities in these guidelines are also outlined. One extremely conservative limit case that is considered in this study is liquefaction as a subsidence problem. All available empirical, phenomenological and stochastic media approaches are reviewed and documented. Using these models, expressions to estimate the maximum differential settlement and rotation are derived. The annual risk versus corresponding rotation values are plotted. The calculation procedures are explained with the help of an example. The model provides information on the relative risk of damage due to earthquake-induced liquefaction between various design alternatives.

PART III–TECHNICAL INFORMATION *(FOR PROGRAM MANAGEMENT USES)*

1. ITEM *(Check appropriate blocks)*	NONE	ATTACHED	PREVIOUSLY FURNISHED	TO BE FURNISHED SEPARATELY TO PROGRAM	
				Check (✓)	Approx. Date
a. Abstracts of Theses	X				
b. Publication Citations		X			
c. Data on Scientific Collaborators		X			
d. Information on Inventions	X				
e. Technical Description of Project and Results		X			
f. Other *(specify)*					

2. Principal Investigator/Project Director Name *(Typed)*	3. Principal Investigator/Project Director Signature	4. Date
Achintya Haldar		

PROBABILISTIC EVALUATION OF DAMAGE POTENTIAL IN EARTHQUAKE-INDUCED LIQUEFACTION IN A 3-D SOIL DEPOSIT

by

Achintya Haldar

Sponsored by

The National Science Foundation
Grant No. CEE-8111691

Report No. SCEGIT-83-117

School of Civil Engineering
Georgia Institute of Technology
Atlanta, Georgia 30332

November, 1983

ACKNOWLEDGEMENTS

This material is based upon work supported by the National Science Foundation under Grant No. CEE-8111691. Any opinions, findings, and conclusions or recommendations expressed in this publication are those of the author and do not necessarily reflect the views of the National Science Foundation.

ABSTRACT

A three-dimensional probabilistic liquefaction model is developed to estimate the risk of damage due to earthquake-induced liquefaction. The model considers the uncertainty in the seismic loading and all the major site-related geotechnical parameters in a liquefaction problem. The scale of fluctuation of a parameter is important input information representing the three-dimensional statistical characteristics of the deposit. Several methods available to calculate the scale of fluctuation are discussed. Some practical alternatives for geotechnical applications are proposed. Damage is defined in terms of differential settlement and rotation in this study. To estimate the allowable values of these parameters, all major codes, standards, and guidelines are reviewed and compared. The deficiencies and non-uniformities in these guidelines are also outlined. One extremely conservative limit case that is considered in this study is liquefaction as a subsidence problem. All available empirical, phenomenological and stochastic media approaches are reviewed and documented. Using these models, expressions to estimate the maximum differential settlement and rotation are derived. The annual risk versus corresponding rotation values are plotted. The calculation procedures are explained with the help of an example. The model provides information on the relative risk of damage due to earthquake-induced liquefaction between various design alternatives.

TABLE OF CONTENTS

Page

LIST OF TABLES

LIST OF FIGURES

Chapter 1

INTRODUCTION

1.1 General Remarks

There are hundreds of recent cases of ground failure and damage to structures due to liquefaction during earthquakes in China, Japan, Yugoslavia, Chile, Central America and the United States. During the 1964 earthquake in Niigata, Japan, many structures settled several feet and suffered up to 80 degrees of tilting (42,43). The same year, in Valdez, Alaska, extensive flow slides washed entire sections of the waterfront into the sea. In 1979, liquefaction caused a considerable amount of damage in Imperial Valley, California (65). Numerous studies have been conducted since then to understand the behavior of cohesionless soil under earthquake loading. Researchers are investigating the causes of the problem; however, the damage associated with liquefaction is a major problem facing an engineer.

To estimate damage during liquefaction, it is necessary to go one step beyond the evaluation of liquefaction potential. Since a volume of sand has to undergo a considerable amount of strain to produce a noticeable amount of damage at the referenced location, it is very important to identify this critical volume. The properties of the soil in this volume also need to be modeled appropriately. It is known that liquefaction does not always lead to damage and that initial deposit conditions affect the extent of damage. Limiting or eliminating damage during liquefaction would be a reasonable criterion for this type of approach. So far, the direct evaluation of damage has not received proper attention.

Considerable error can be incurred during the estimation of damage. This necessitates the availability of a simple but efficient and practical probabilistic model to study the risk of damage associated with the liquefaction phenomenon.

1.2 Objectives and Scope of Study

This study will be limited to earthquake-induced liquefaction. The estimation of damage during earthquake-induced liquefaction is a very complex problem and needs to be developed in several stages. Haldar and Miller (28) developed a three-dimensional probabilistic model considering the uncertainties in the load and resistance models. The load model considers the uncertainty in the seismic loading. The resistance model includes the uncertainty associated with the laboratory estimation as well as the field estimation of a geotechnical parameter. This model is developed further and the statistical techniques are modified further to represent the in situ conditions more accurately.

Damage is a subjective parameter, and is a very controversial subject. Thus, it is extremely important to define damage and the corresponding damage criterion. These are defined in this study from an extensive literature review. A very preliminary model is developed to evaluate the risk of damage from earthquake-induced liquefaction corresponding to the damage criterion discussed above. This damage model will be developed further in a subsequent study.

1.3 Report Organization

In Chapter 2, the three-dimensional probabilistic model proposed by Haldar and Miller (28) is developed further. Some statistical techniques

required to model the parameters in this model are discussed. The scale of fluctuation is an important parameter. Several methods available to evaluate the scale of fluctuation are discussed and modified whenever possible for geotechnical applications.

Chapter 3 is devoted to defining damage and the damage criterion. Several measures of damage are discussed. Most of the commonly used codes, standards, guidelines and text books are compared and their limitations are documented. After an extensive literature review, some recommendations are made on allowable settlement, differential settlement, and rotation values.

A subsidence model is used in this study to evaluate risk of damage in earthquake-induced liquefaction. All available subsidence prediction models including empirical, phenomenological and stochastic media approaches are reviewed and documented in Chapter 4. Using these models, procedures to estimate the maximum settlement, maximum differential settlement, maximum slope and rotation are developed and related to the corresponding allowable values.

The discussions made in Chapters 2 through 4 are put together in Chapter 5 and the annual risk of damage to a site from the liquefaction of a volume of sand during an earthquake is estimated. The steps involved are explained with an example.

The summary and principal conclusions are presented in Chapter 6.

Chapter 2

PROBABILISTIC LIQUEFACTION MODEL

2.1 General Remarks

The availability of a simple but efficient probabilistic liquefaction model is necessary to evaluate damage associated with earthquake-induced liquefaction.

The estimation of liquefaction potential does not lead to the estimation of damage due to liquefaction. To estimate the damage during liquefaction, it is necessary to go one step beyond the evaluation of liquefaction potential. A volume of sand has to undergo a considerable amount of strain to produce a noticeable amount of damage at the referenced location. It is very important to identify this critical volume. Soil properties in this critical volume need to be modeled appropriately. Moreover, liquefaction does not always lead to damage and the initial deposit conditions affect the extent of damage. Considering all the aforementioned information, it is appropriate to develop a comprehensive liquefaction model considering damage as the design criterion.

This study will be limited to earthquake-induced liquefaction. "Cyclic mobility" would be the most appropriate definition of the problem under consideration according to the most recent literature (47). However, the term "liquefaction" will be used in this study instead of "cyclic mobility" since the former is the most widely used by practicing engineers.

There is general agreement about the mechanism by which the onset of liquefaction occurs during an earthquake. The basic cause of liquefaction in a saturated cohesionless soil deposit during an earthquake is the buildup of pore water pressure due to the application of cyclic shear

stresses induced by the ground motion. The cohesionless soil tends to become more compact while the soil structure rebounds to the extent necessary to keep the volume constant. This interplay of volume reduction and soil structure rebound determines the magnitude of the increase in pore water pressure. If sufficient pore water pressure is produced, the effective stress becomes zero and the deposit assumes the characteristics of a viscous liquid. This essentially leads to liquefaction.

The basic causes of liquefaction appear to be simple. However, it is a very complex problem. Quite a few factors influence the liquefaction potential evaluation. Moreover, each factor influences the evaluation to a different degree. For proper evaluation, information on soil properties affecting the liquefaction phenomenon and earthquake loading needs to be available. The estimation of in situ soil parameters can be obtained by measuring them directly in the deposit, or indirectly from empirical relationships or by measuring them in the laboratory using so-called "undisturbed" samples. Considerable error can be incurred during these processes (12,14,22,31,32,35,36). The nonhomogeneity of the soil properties in the liquifiable volume has to be modeled in three dimensions (58). Long-distance fluctuations and local variations in soil properties can only be modeled effectively using probability theory. Seismic loading is also unpredictable (13,15). This necessitates the availability of a simple but efficient and practical probabilistic model to study the risk of damage associated with the liquefaction phenomenon. There are several probabilistic liquefaction models available in the literature (12,16,17,18, 27,29,64). Their merits and demerits are discussed elsewhere by Haldar and Miller (28). Haldar and Miller (28) developed a basic working model

earlier. This model is developed further and is discussed in the following sections.

2.2 Deterministic Liquefaction Model

The risk of liquefaction of a soil deposit can be estimated by comparing the in situ shear resistance of a soil element τ_R and the average equivalent uniform shear stress of intensity τ_A that will act on the soil element for N_{eq} number of cycles during an earthquake. Liquefaction will occur when τ_A is greater than τ_R. τ_A and τ_R can be estimated using a concept similar to that of Seed and Idriss (48). Haldar and Miller (28) discussed this concept in great detail.

τ_A can be estimated from the following relationship:

$$\tau_A = S_L \, r_d \, \gamma_s \, h \, \frac{a_{max}}{g} \tag{2.1}$$

in which S_L = stress ratio to convert the maximum applied shear stress to the uniform shear stress, τ_A, and can be considered as 0.75 (32); r_d = the stress reduction coefficient to consider the flexibility of the soil column under consideration; γ_s = the saturated unit weight of the soil; g = the acceleration due to gravity; and a_{max} = the design maximum ground acceleration.

Haldar and Miller (28) showed that the shear resistance, τ_R, mobilized by an element of soil during earthquake shaking can be modeled effectively by introducing the shear strength parameter R such that

$$R = \frac{\tau_R}{\sigma'_m D_r} \tag{2.2}$$

in which σ'_m = the average effective normal stress and D_r = the relative

density. The R parameter was introduced by Haldar and Tang (30). σ'_m can be estimated as

$$\sigma'_m = \frac{\sigma'_1 + \sigma'_2 + \sigma'_3}{3} \tag{2.3}$$

in which σ'_1, σ'_2, and σ'_3 are the effective stresses in three directions at a point in the deposit. The in situ value for R can be inferred from laboratory test results if the value for R measured in the laboratory is modified by a corrective factor, C_r, i.e.

$$R_{field} = C_r \cdot R_{lab} \tag{2.4}$$

Combining Equations 2.2 and 2.4, the following expression can be obtained:

$$\tau_R = C_r \cdot R \cdot \sigma_m \cdot D_r \tag{2.5}$$

2.3 Three-Dimensional Probabilistic Liquefaction Model

The liquefaction potential of a soil deposit can be evaluated if information on the various parameters in Equations 2.1 through 2.5 is available. However, considerable error can be incurred in estimating these parameters. All the parameters mentioned are uncertain to some degree and should therefore be modeled as random variables.

In addition, soil parameters typically exhibit local variations about their average values or about major trends (horizontally and vertically). Thus, an evaluation of the liquefaction potential of the deposit at the so-called "weakest point" may be misleading. As discussed earlier, a sufficient volume of sand has to undergo a considerable amount of strain in order to produce a noticeable amount of damage at the referenced location. This critical volume may contain pockets of very loose as well as very dense sand. Evaluation of the liquefaction potential of this volume of

sand considering either the loose or dense pocket will obviously be incomplete. The soil property averaged over the volume would be more representative than the point estimate. Thus, τ_A and τ_R in Equations 2.1 and 2.2, respectively, need to be modeled in terms of spatial averages. Taking the spatial average of τ_R over a volume Δv yields:

$$\tau_{R_{\Delta v}} = \frac{1}{\Delta v} \int_{\Delta x} \int_{\Delta y} \int_{\Delta z} \tau_R (x,y,z)\, dx\, dy\, dz \tag{2.6}$$

in which $\tau_{R_{\Delta v}}$ = the spatial average over the volume Δv, $\Delta v = \Delta x \cdot \Delta y \cdot \Delta z$, and Δx, Δy, Δz are the lengths of the soil volume in the x, y and z directions, respectively. However, $\tau_{R_{\Delta v}}$ is random. Using first-order approximate analysis and assuming a statistically homogeneous soil deposit, Haldar and Miller (28) showed that the mean value of τ_R can be estimated as

$$\tau_{R_{\Delta v}} = \mu_{\tau_R} = \mu_{C_r} \cdot \mu_R \cdot \mu_{\sigma'_m} \cdot \mu_{D_r} \tag{2.7}$$

where μ represents the point mean. The three-dimensional characteristics of the relative density in a deposit are expected to be more important than the other parameters. Modeling only D_r in three dimensions (other parameters can be modeled similarly) and assuming statistical independence among parameters, Haldar and Miller (28) estimated the variance of $\tau_{R_{\Delta v}}$ as:

$$\text{Var}\,(\tau_{R_{\Delta v}}) = \mu^2_{\tau_R} \left[\Omega^2_{N_{\tau_R}} + \Omega^2_{C_r} + \Omega^2_R + \Omega^2_{\sigma'_m} + \Gamma^2_{D_{r_x}}(\Delta x) \cdot \Gamma^2_{D_{r_y}}(\Delta y) \cdot \Gamma^2_{D_{r_z}}(\Delta z) \cdot \Omega^2_{D_r} \right] \tag{2.8}$$

in which Ω represents the point coefficient of variation (COV) and $\Omega_{N_{\tau_R}}$ is the modeling error. $\Gamma^2_{D_{r_x}}(\Delta x)$, $\Gamma^2_{D_{r_y}}(\Delta y)$, and $\Gamma^2_{D_{r_z}}(\Delta z)$ are called the

variance functions of D_r in the x, y, and z directions, respectively. They describe the decay of the variance of the spatial average of D_r as the averaging dimensions increase (58,59).

For all practical purposes, the variance function in the x direction can be estimated as

$$\Gamma^2_{D_{r_x}}(\Delta x) \doteq \begin{cases} 1.0; \ \Delta x \leq \theta_{D_{r_x}} \\ \dfrac{\theta_{D_{r_x}}}{\Delta x}; \ \Delta x > \theta_{D_{r_x}} \end{cases} \tag{2.9}$$

where $\theta_{D_{r_x}}$ is the scale of fluctuation in the x direction. It is discussed further in Section 2.5. The variance functions in the y and z directions can be estimated similarly knowing $\theta_{D_{r_y}}$ and $\theta_{D_{r_z}}$. Methods available to estimate the scale of fluctuation are discussed in Section 2.6.

In a similar manner, the spatial average of τ_A over the volume Δv is given by

$$\tau_{A_{\Delta v}} = \frac{1}{\Delta v} \int_{\Delta x} \int_{\Delta y} \int_{\Delta z} \tau_{A_{\Delta v}}(x,y,z) \, dx \, dy \, dz \tag{2.10}$$

The predictive model of τ_A is given by Eq. 2.1. Though a_{max} and r_d are random variables, their spatial variability can be considered negligible. The spatial variability of γ_s will not be considered directly here; however, it is considered indirectly in the spatial variability of D_r. Thus, for a liquifiable volume Δv, the spatial mean and variance of $\tau_{A_{\Delta v}}$ becomes

$$\overline{\tau}_{A_{\Delta v}} = \mu_{\tau_A} = S_L \, \mu_{r_d} \, \mu_{\gamma_s} \cdot h \frac{\mu_{a_{max}}}{g} \tag{2.11}$$

$$\text{Var}(\tau_{A_{\Delta v}}) = \mu^2_{\tau_A} \, \Omega^2_{\tau_A} = \mu^2_{\tau_A} \left[\Omega^2_{r_d} + \Omega^2_{\gamma_s} + \Omega^2_{a_{max}} \right] \tag{2.12}$$

The values of g, S_L and h are assumed to be known.

The probability that the soil volume Δv will liquefy is given by the probability of the event $\tau_{R_{\Delta v}} \leq \tau_{A_{\Delta v}}$. Since the statistics of $\tau_{A_{\Delta v}}$ and $\tau_{R_{\Delta v}}$ cannot be adequately defined beyond the first two moments, for simplicity, lognormal distributions can be prescribed for $\tau_{A_{\Delta v}}$ and $\tau_{R_{\Delta v}}$ in estimating the probability of liquefaction. The validity of these probability estimates was studied by Haldar (24). The probability of liquefaction is thus given by the following:

$$P_{f_{\Delta v}} = 1 - \Phi\left(\frac{\ln\left[\frac{\mu_{\tau_{R_{\Delta v}}}}{\mu_{\tau_{A_{\Delta v}}}}\sqrt{\frac{1+\Omega_{\tau_{A_{\Delta v}}}^2}{1+\Omega_{\tau_{R_{\Delta v}}}^2}}\right]}{\sqrt{\ln\left[(1+\Omega_{\tau_{R_{\Delta v}}}^2)(1+\Omega_{\tau_{A_{\Delta v}}}^2)\right]}}\right) \tag{2.13}$$

where $\Phi(\ )$ is the standard normal cumulative distribution function.

Equation 2.13 can be used to estimate the risk of liquefaction in a volume of sand when both the maximum ground acceleration and the earthquake magnitude at a site are known.

To design a site against future earthquakes where a_{max} and N_{eq} or earthquake magnitude M are unknown, the uncertainties in these parameters need to be incorporated in Eq. 2.13. Using the theorem of total probability, Haldar and Tang (30) showed that the probability of liquefaction of a soil volume can be calculated as

$$P_f = \int_{(n_{eq})_o}^{(n_{eq})_u} \int_{0}^{a_{max}} (P_{f_{\Delta v}}\ a_{max}, n_{eq})\ f_{A_{max}}(a_{max})\ f_{N_{eq}}(n_{eq})\ da_{max}\ dn_{eq} \tag{2.14}$$

in which $f_{A_{max}}(a_{max})$ and $f_{N_{eq}}(n_{eq})$ are the density functions of A_{max} and N_{eq}, respectively. $(n_{eq})_u$ and $(n_{eq})_o$ are the values of N_{eq} corresponding to the upper and lower bound magnitudes of the earthquakes. The conditional probability, $(P_{f_{\Delta v}} \mid a_{max}, n_{eq})$ can be estimated using Eq. 2.13.

2.4 Uncertainty Analysis of Parameters

To evaluate Eq. 2.13 or 2.14, the uncertainty associated with all the parameters mentioned in Section 2.3 need to be available in terms of mean and coefficient of variation. Haldar and Miller (28) evaluated these in the previous study. It is a very complex problem and will not be repeated here for the sake of brevity. Ref. 28 is widely available and can be consulted for further detail. However, some qualitative discussion is necessary here for the sake of completeness.

The uncertainty associated with the estimation of the in situ relative density contributes significantly to the overall uncertainty in τ_R. The amount of uncertainty in D_r depends on how it was determined; directly using the information on the maximum, minimum and inplace dry densities, or indirectly using a correlation between the Standard Penetration Test (SPT) value and D_r values. Haldar and Tang (31) observed that, using the direct method, the uncertainties in D_r in terms of COV could be of the order of 0.11 to 0.36. When the indirect method is used, Haldar and Miller (28) observed that the uncertainty could be of the order of 0.20 to 0.35. The uncertainty associated with the shear strength parameter R is also considerable. Using large-scale shaking table test results on liquefaction and considering factors such as system compliance, methods of sample preparation, mean grain size, multidirectional shaking and other secondary factors, Haldar and Miller (28) evaluated the probabilistic characteristics

of R. The uncertainty associated with the prediction of the in situ value of R could be of the order of 0.20 to 0.30.

The uncertainty associated with the load parameters is also considerable. The magnitude and duration of the future earthquake, as well as the maximum ground acceleration at a particular site within a specified time period need to be considered probabilistically. Available geological, seismological and observed records at or near the region concerned need to be considered in estimating the seismic risk of the region. The uncertainty associated with the attenuation equations themselves could be of the order of 0.90 in terms of COV (15). Haldar and Tang (32) discussed the uncertainty associated with N_{eq}, the equivalent number of uniform stress cycles corresponding to a design earthquake magnitude. Considering all the relevant information, the seismic risk of a site in terms of design acceleration versus return period can be developed.

2.5 Scale of Fluctuation

The scale of fluctuation shows relatively strong correlation of persistence from point to point. A small value implies rapid fluctuations about the average, while large values suggest that a slowly varying component is superimposed on the average value. The scale of fluctuation can also provide a host of practical information for the site exploration problem; for example, to avoid wasteful redundancy in information gathering, sampling distances should be chosen in such a way that they are large in comparison with the scale of fluctuation. On the other hand, when a soil property is being determined by two different tests, the locations of pairs of samples should be well within the correlation distance for maximum effectiveness.

2.6 Evaluation of Scale of Fluctuation

Several methods are available to estimate the scale of fluctuation. The scale of fluctuation, θ, in any direction (any of the two horizontal and one vertical) can be theoretically estimated by using the random field theory. It can be estimated from the information on variance function, correlation function and the unit area one-sided spectral density function (23,26,59).

2.6.1 Scale of fluctuation using variance function

Consider X(t) as a stationary random process. Averaging X(t) over a duration T, a family of moving average processes $X_T(t)$ can be obtained as:

$$X_T(t) = \frac{1}{T} \int_{t-T/2}^{t+T/2} X(u)\, du \tag{2.15}$$

The variance of $X_T(t)$ can be shown to be:

$$\text{Var}\,(X_T) = \Gamma(T)\, \sigma^2 \tag{2.16}$$

in which $\Gamma(T)$ is the variance function of X(t) and σ^2 is the point variance. Knowing the variance function, the scale of fluctuation θ can be estimated as

$$\theta = \lim_{T \to \infty} T\Gamma(T) \tag{2.17}$$

2.6.2 Scale of fluctuation using correlation function

Correlation function $\rho(\tau)$ represents the correlation structure of two points of X(t) separated by τ in a nondimensional way. The relationship between $\Gamma(T)$ and $\rho(\tau)$ can be shown to be

$$\Gamma(T) = \frac{2}{T} \int_0^T (1 - \frac{\tau}{T})\ \rho(\tau)\ d\tau \qquad (2.18)$$

The scale of fluctuation in this case can be shown to be:

$$\theta = 2 \int_0^\infty \rho(\tau)\ d\tau \qquad (2.19)$$

2.6.3 Scale of fluctuation using one-sided spectral density function

When the stationary random process X(t) is represented in the frequency domain, it produces a spectral density function, $S(\omega)$. Since $S(\omega)$ is symmetric about $\omega=0$, it can be expressed as a one-sided spectral density function $G(\omega)$ for $\omega \geq 0$. When $G(\omega)$ is normalized with respect to σ^2 mentioned earlier, it produces a unit area one-sided spectral density function, $g(\omega)$. In this case, the scale of fluctuation can be estimated as

$$\theta = \pi\ g(\omega) \quad ; \quad \text{when } \omega = 0 \qquad (2.20)$$

2.6.4 Scale of fluctuation for geotechnical problems

For a geomechanics problem, Eqs. 2.17, 2.19, and 2.20 cannot be used because $\Gamma(T)$, $\rho(\tau)$ and $g(\omega)$ may not be known. The only information available is a series of borings data. In this case, the h-step variance function can be estimated as

$$\Gamma(h) = \frac{1}{(\ell-h+1)} \sum_{a=1}^{\ell-h+1} \left\{ \frac{1}{m} \sum_{j=1}^{m} \left[\sum_{i=a}^{h+a-1} u_j'(i) \right]^2 - \left[\frac{1}{m} \sum_{j=1}^{m} \sum_{i=1}^{h+a-1} u_j'(i) \right]^2 \right. \qquad (2.21)$$

in which ℓ is the number of layers in the deposit, h is the averaging interval, m is the number of borings, $u_j(i)$ is the transformed soil property in the ith layer and jth boring = $u_j(i)$ - trend in (i), $u_j(i)$ is the soil property in the ith layer and jth boring.

2.6.5 Some practical approaches

The concept of coefficient of correlation between values of u(t) at two points can be used to estimate the scale of fluctuation for geotechnical applications. When points are located at very small intervals, the correlation coefficient will be close to 1, and it usually decays as the distance increases. For an assumed theoretical correlation model (58), the scale of fluctuation can be estimated. Another approximate method can be used to estimate θ if a reasonably complete record of u(t) is available. It is based on the approximate relationship between the scale of fluctuation and the average distance, d, between the intersections of the fluctuating property, u(t), and its mean. The average distance between mean crossings is approximately (58):

$$\overline{d} \simeq \frac{\pi}{2} \cdot \theta \simeq 1.25\ \theta \tag{2.22}$$

A deposit could have three different scales of fluctuation in the three different directions. For many sites, the scales of fluctuation in the two horizontal directions would be the same. The information on the scale of fluctuation could be used to estimate the statistics of spatially averaged soil properties.

2.7 Conclusions

The three-dimensional probabilistic model described here is used to evaluate the damage associated with earthquake-induced liquefaction. The

detailed uncertainty analysis of the parameters is not given here for the sake of brevity but is widely available in the literature.

Chapter 3

DAMAGE CONSIDERATION

3.1 General Remarks

Earthquake-induced liquefaction causes damage to structures and property and is of major concern to engineers. The most common types of damage that can be expected due to liquefaction following an earthquake are settlement, differential settlement, subsidence, and tilting of a structure at the site.

Damage is an extremely controversial subject due to its qualitative nature. However, in engineering design this subject must be addressed. This is usually done by assigning allowable values for the damage measurements (settlement, differential settlement and rotation) as given in codes, design guidelines, and the literature. It is quite logical to assume that the same standards should also be used for assessing liquefaction damage. However, the adequacy of the presently available codes or standards in this area needs to be addressed, and will be discussed in the following sections. The problem is even further complicated for damage associated with earthquake-induced liquefaction, because it depends on the volume of the liquefied zone, the depth of the liquefied volume below the ground surface, the initial site conditions in terms of denseness or looseness, the size and type of foundation, the intensity of earthquake motion at the site, etc. (25). Generally, codes do not address the damage measurement in terms of all the aforementioned parameters.

Damage will be defined in this study in terms of differential settlement or rotation. Other damage criteria will be addressed in a subsequent study.

The amount of settlement, differential settlement or rotation that will cause damage to a structure is difficult to determine analytically. In the first place, damage, by its very nature, is a subjective concept and, therefore, very difficult to assess quantitatively. Even if damage to a structure is somehow associated with cracking, as is usually done, determination of the amount of foundation deformation that will cause a particular level of cracking in structural or non-structural members is an extremely complicated problem. This is not amenable to the usual methods of structural analysis (61). For these reasons, allowable settlement is usually determined empirically, based on observations of settlement and damage in existing buildings.

In this chapter, all the information on allowable settlement, differential settlement and rotation of structures available in the codes, the design guidelines and in the literature is summarized. Based on this information, the damage criterion most appropriate for assessing the damage caused by earthquake-induced liquefaction is recommended.

3.2 Measures of Settlement

Some of the common terminology that is used to describe foundation settlement is illustrated in Fig. 3.1 where a foundation is shown to settle from points ABCDE to A'B'C'D'E'. S_i is defined as the absolute settlement or subsidence at point i, and δ_{ij} is the differential settlement between points i and j. δ_{ij} is usually computed as $\delta_{ij} = S_i - S_j$. S_o and ω are the uniform settlement and rigid body tilt of the foundation, respectively. Δ is the relative deflection and is defined as the maximum displacement measured from a straight line connecting two reference points.

The amount of damage to the structure caused by the foundation settlement depends on the uniformity of the settlement. If each point of

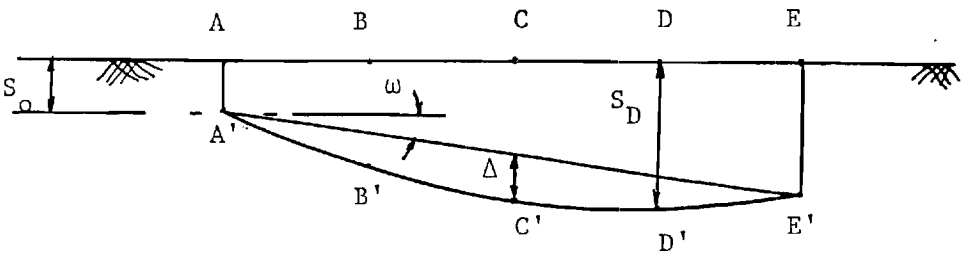

Fig. 3.1 Foundation Settlement

the foundation settles the same amount, the structure will not be damaged (52). Furthermore, many authors believe that the structure is not affected by a rigid body tilt of the foundation, although limits on the magnitude of the rigid body tilt may be imposed for purely aesthetic reasons (11,21,51, 61). Leonards (37) disagrees with this assumption; he suggests that rigid body tilt affects the stresses and strains in a framed structure supported on isolated spread footing and should, therefore, be included in the settlement criteria. For these reasons, most authors use, as an index of critical settlement, the angular distortion, β_{ij}, which is computed as

$$\beta_{ij} = \delta_{ij}/l_{ij} - \omega \tag{3.1}$$

where l_{ij} is the distance between points i and j. It is clear that uniform settlement and rigid body tilt are removed with this measure of settlement.

Skempton and MacDonald (51) have suggested that the radius of curvature is the settlement characteristic that is most indicative of cracking. However, the radius of curvature cannot be readily evaluated in a typical settlement investigation. Instead, it has been suggested that the deflection ratio, Δ/L, which is computed as the relative deflection divided by the length of the foundation, be used as the critical index of settlement since it is an approximate measure of the curvature (11,61). The USSR Building Code has based the allowable settlement criterion for masonry structures on Δ/L, but in the U.S., the angular distortion, β, is preferred as a critical index of settlement (45,61).

3.3 Burland and Wroth Beam Analogy

Burland and Wroth (11) point out that most of the damage due to foundation settlement is confined to cladding, panels and finishes rather than structural elements. Damage to cladding, panels and finishes is manifested as cracking of the material, and the onset of visible cracking

may be associated with a critical value of tensile strain, ε_{crit}. To relate foundation settlement characteristics to cracking in nonstructural elements, Burland and Wroth (11) suggest that the building may be approximately represented as a simply supported rectangular beam (Fig. 3.2). It is assumed that elementary beam theory can be used to calculate stresses and strains in the beam up to the onset of cracking, and that the material behavior is linearly elastic, homogeneous and isotropic. Indeed, this simple beam idealization is an oversimplification of real building behavior, but as Burland and Wroth commented, "the study of a simple beam does help to illustrate a number of important features."

Using this beam analogy, a relationship between the deflection ratio and critical tensile strain can be developed. Two cases must be considered; a case where Δ/L is limited by the onset of cracking due to direct tensile strain, and a case where Δ/L is limited by the onset of cracking due to diagonal tensile strain. These relationships are given by the following expressions for a uniformly distributed load over the entire span length (61).

$$(\Delta/L) = \left[\frac{5}{24} \left(\frac{L}{H}\right) + \frac{1}{4} \left(\frac{E}{G}\right) \left(\frac{H}{L}\right)\right] \varepsilon_{crit} \qquad (3.2)$$

when direct tensile strain is critical, and

$$(\Delta/L) = \left[\frac{5}{6} \left(\frac{L}{H}\right)^2 \left(\frac{G}{E}\right) + 1\right] \varepsilon_{crit} \qquad (3.3)$$

when diagonal tensile strain is critical. L and H are, respectively, the length and height of the building, and E and G are, respectively, the equivalent elastic and shear modulus. Estimation procedures for ε_{crit}, for both the direct tensile strain and the diagonal tensile strain, are

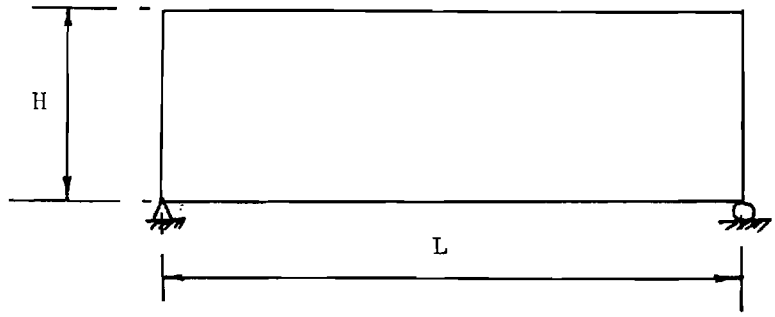

Simple Beam Representation

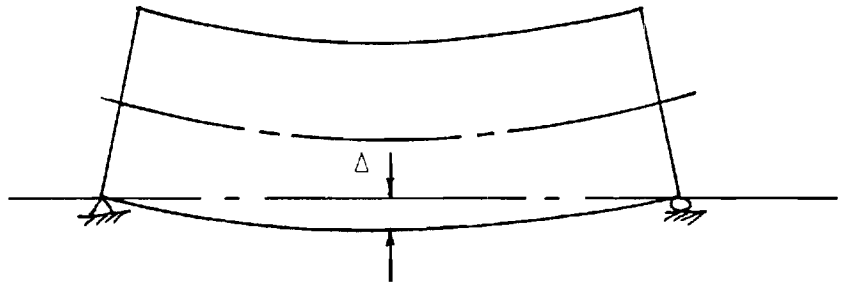

Deflected Shape

Fig. 3.2 Burland and Wroth Beam Analogy

discussed by Wahls (61) elsewhere. Eqs. 3.2 and 3.3 are plotted in Fig. 3.3.

Considering Fig. 3.3, the following observations can be made regarding allowable settlement in buildings:

(1) The L/H ratio may be interpreted as a measure of building flexibility;

(2) Diagonal tensile strain is critical in the case of very rigid buildings; otherwise, direct tensile strain controls the allowable values of Δ/L;

(3) Flexible buildings can tolerate higher values of Δ/L than rigid buildings;

(4) The E/G ratio may be interpreted as the equivalent longitudinal stiffness of the building relative to the equivalent shear stiffness;

(5) Diagonal tensile strains become more critical as the equivalent longitudinal stiffness increases or the equivalent shearing stiffness decreases.

Wahls (61) suggests that the behavior of framed structures, which are relatively flexible in shear, and reinforced load-bearing walls, which are relatively stiff in direct tension, may be approximated by a rectangular beam with a high E/G ratio. The behavior of unreinforced masonry walls and structures, which have relatively low tensile resistance, in the sagging mode (settlement curve concave upward) may be approximated by a rectangular beam with an E/G ratio equal to 2.6. The same unreinforced masonry in the hogging mode (settlement curve concave downward) may be represented by a rectangular beam with the neutral axis located at the bottom of the beam and a very low E/G ratio.

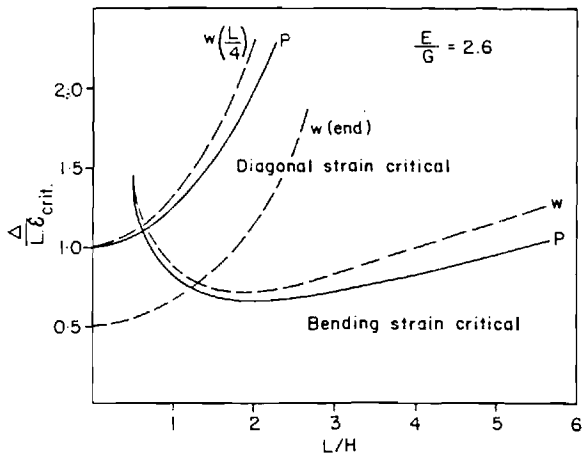

Fig. 3.3 Relation of $\Delta/L\ \varepsilon_{crit}$ to L/H for Isotropic Beam-Neutral Axis at Mid-Depth (61)

3.4 Empirical Studies

Although the simple beam analogy discussed in the previous section is useful for illustrative purposes, the behavior of a real structure is much more complicated. Many factors affect the allowable settlement of structures, such as type and size of the structure, properties of the structural materials, properties of the nonstructural materials, type of foundation, properties of the subsurface soil and rate of settlement. For these reasons, almost all of the guidelines dealing with allowable settlement of structures are based on empirical studies of settlement and damage in existing structures (61).

In the classic empirical study on allowable settlement of structures, Skempton and MacDonald (51) compiled data on the occurrence or nonoccurrence of damage and the associated value of the angular distortion in 98 buildings. Only load-bearing wall structures and steel or reinforced concrete frame structures with masonry panel walls and partitions were included in the study. There was no data available for framed structures with curtain walling or dry wall partitions. Settlement damage in the frame structures was classified as either (1) architectural damage which involved cracks in wall panels, ceilings, floors and finishes, (2) structural damage which involved excessive distortion of the structural frame, or (3) a combination of architectural and structural damage. Cracking of the walls was designated as damage in load-bearing wall structures.

Based on an analysis of the data, Skempton and MacDonald (51) made the following observations:

(1) The behavior of wall panels and nonstructural elements determine the allowable settlement in frame structures,

(2) Cracking is likely to occur in load-bearing walls and in the panel walls of frame structures if the angular distortion exceeds 1/300,

(3) Structural damage is likely to occur in beams and columns if the angular distortion exceeds 1/150,

(4) Building and foundation type does not seem to affect the limiting value of the angular distortion causing damage,

(5) Soil type does not have a major effect on the allowable values of angular distortion, although somewhat larger values can be tolerated by structures founded on soils that settle at a slower rate.

(6) Angular distortion is more reliable as an indicator of damage than either maximum settlement or maximum differential settlement.

In a more recent empirical study of 95 additional cases of settlement data, Grant et al. (21) confirmed Skempton and MacDonald's conclusions, but they suggested that the settlement rate has less of an effect on allowable values than was originally believed.

3.5 Guidelines Regarding Allowable Settlements

Guidelines regarding allowable values of foundation settlement are given in a number of building codes (1,2,3,4,5,34,40). In addition, several authors have recommended their own allowable values (9,44,45,52,56). For the most part, these values are based on theoretical treatments, similar to Burland and Wroth's (11) study, empirical treatments, and personal experience and intuition. Terzaghi and Peck (56) wrote, "Most ordinary structures, such as office buildings, apartment houses, or factories, can withstand a differential settlement between adjacent columns of three quarters of an inch." Considering that a typical column span at that time was 20', the allowable angular distortion recommended by Terzaghi and Peck was 1/320, a value close to Skempton and MacDonald's. Peck,

Hanson and Thornburn (44) recommended an allowable differential settlement of 3/4" between columns, but they commented that this limit would be different depending on the structural type or structural material.

More extensive guidelines on allowable settlement have been suggested by Sowers (52), Bjerrum (9) and Polshin and Tokar (45). These are listed in Tables 3.1, 3.2 and 3.3, respectively. Bjerrum's allowable values are based on Skempton and MacDonald's study. The safe limit for no cracking of buildings, $\beta = 1/500$, was suggested by Skempton and MacDonald as a design criterion that provides some factor of safety against cracking (51). Polshin and Tokar's settlement criteria are from the USSR Building Code. The limiting values are approximately the same as Bjerrum's except that load-bearing wall structures are treated differently. The settlement criterion for these structures is in terms of the deflection ratio, Δ/L. Allowable values were established by theoretically relating Δ/L to the critical tensile strain, ε_{crit} in a manner similar to Burland and Wroth's (11). Sowers' allowable values do not seem to be much different than Bjerrum's or Pulshin and Tokar's.

Building codes in the U.S. are far less informative regarding settlement criteria. Most codes stipulate that the effects of differential settlement should be considered in the structural design, for example the Building Code Requirements for Reinforced Concrete (ACI 318-77) (2), Article 9.2.7, dictates that, "Where structural effects T of differential settlement, creep, shrinkage, or temperature change may be significant in design, required strength U shall be at least equal to $U = 0.75 (1.4D + 1.4T + 1.7L)$". However, the tolerance of a structure to settlement is determined, in most cases, by the behavior of the non-structural elements - serviceability rather than strength should be the consideration.

Table 3.1 Allowable Settlement According to Sowers (52)

Type of Movement	Limiting Factor	Maximum Settlement
Total settlement	Drainage and access	0.15 to 0.6 m (0.5 to 2 ft)
	Probability of differential settlement	
	Masonry walls	25 to 50 mm (1 to 2 in.)
	Framed buildings	50 to 100 mm (2 to 4 in.)
Tilting	Tower, stacks	$0.004B$†
	Rolling of trucks, stacking of goods	$0.01S$†
	Crane rails	$0.003S$†
Curvature	Brick walls in buildings	$0.0005S$ to $0.002S$†
	Reinforced concrete building frame	$0.003S$†
	Steel building frame, continuous	$0.002S$†
	Steel building frame, simple	$0.005S$†
Maximum permissible settlement	Front slab, 100 mm thick	$0.02S$†

* B is base width; S is column spacing.
† Differential settlement in distance B or S.

Table 3.2 Allowable Settlement According to Bjerrum(9)

Category of potential damage (1)	$\beta = \delta/\ell$ (2)
Danger to machinery sensitive to settlement	1/750
Danger to frames with diagonals	1/600
Safe limit for no cracking of buildings[b]	1/500
First cracking of panel walls	1/300
Difficulties with overhead cranes	1/300
Tilting of high rigid buildings becomes visible	1/250
Considerable cracking of panel and brick walls	1/150
Danger of structural damage to general buildings	1/150
Safe limit for flexible brick walls, $L/H > 4$[b]	1/150

[b] Safe limits include a factor of safety.

Table 3.3 Allowable Settlement According to Polshin and Tohar (45)

Type of structure (1)	Sand and hard clay (2)	Plastic clay (3)
(*a*) $\beta = \delta/\ell$		
Civil- and Industrial-Building Column Foundations:		
For steel and reinforced concrete structures	0.002	0.002
For end rows of columns with brick cladding	0.007	0.001
For structures where auxiliary strain does not arise during nonuniform settlement of foundations	0.005	0.005
Tilt of smokestacks, towers, silos, etc.	0.004	0.004
Craneways	0.003	0.003
(*b*) Δ/L		
Plain brick walls:		
For multistory dwellings and civil buildings		
at $L/H \leq 3$	0.0003	0.0004
at $L/H \geq 5$	0.0005	0.0007
For one-story mills	0.0010	0.0010

Although most of the major codes in the U.S., i.e., American Institute of Steel Construction (AISC) (1), American Concrete Institute (ACI) (2), American Association of State Highway and Transportation Officials (AASHTO) (3), American National Standard Institute (ANSI) (4), International Conference of Building Officials, Uniform Building Code (UBC) (34), and Applied Technology Council (ATC) (5) do not stipulate specific allowable settlement criteria; they do recommend serviceability limits. It is reasonable to assume that the same standards should also apply to foundation settlement. Table 3.4 lists the serviceability requirements of the major U.S. codes. Limits specified for building construction, i.e. AISC, ACI, and UBC, are approximately the same and are based on the tolerance of plaster ceilings and panel walls to deflections. The AASHTO serviceability limits for bridge construction are somewhat more stringent. The ANSI and ATC codes do not specify settlement or serviceability limits. The Naval Facilities Engineering Command (40) NAVFAC DM-7.1 is the only code found by this writer that explicitly stipulates settlement limits. These guidelines are shown in Fig. 3.4.

3.6 Conclusions

In this chapter several aspects of foundation settlement and the damage associated with settlement are discussed. It was seen that damage is a very subjective concept and, therefore, very difficult to relate to a measure of settlement. Empirical and theoretical studies showed that the angular distortion, β, is well correlated with the level of cracking in panel walls of frame structures, whereas the deflection ratio , Δ/L, is better for load-bearing wall structures. Allowable values of these settlement parameters recommended by the major codes, design guidelines, and in the literature are presented.

Table 3.4 Allowable Deformations

Settlement Measure	AISC	ACI	AASHTO	ANSI	UBC	ATC3-06/ NBSSP-510	NAVFAC DM-7.1
S_{max}	-	-	-	-	-	-	-
δ_{max}	-	-	-	-	-	-	Fig.3.7
$\beta=(\delta/\ell)-\omega$	-	-	-	-	-	-	-
(Δ/L)	1/360	1/480	1/800	-	1/360	-	-
Comments	AISC Sect. 1.13.1 deflection limit due to live load, established for floor beams supporting plastered ceilings, serviceability	ACI Sect. 9.5 - roof or floor construction supporting or attached to nonstructural elements likely to be damaged by large deflections, serviceability Control of Deflections	AASHTO Sect. 1.7.6 deflection due to service load plus impact Deflection		UBC Sect. 2307 roof members supporting plaster and floor member (Loaded with LL only) Maximum Allowable Deflection for Structural Members		NAVFAC DM-7.1 Sect. 3 Tolerable Settlement

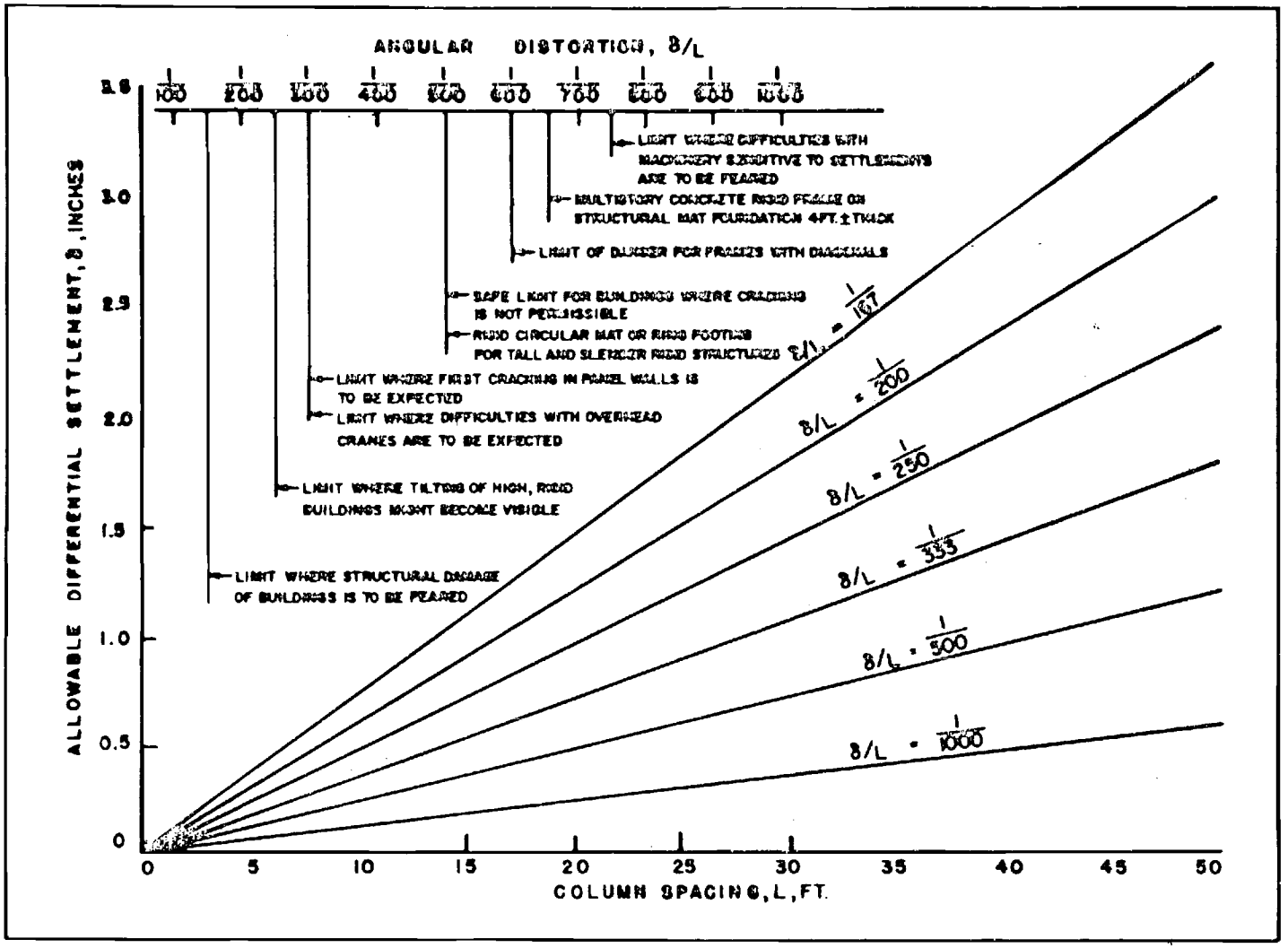

Fig. 3.4 Allowable Settlement for Buildings (NAVFAC DM-7.1) (40)

It is difficult to arrive at a consensus on the most suitable settlement criterion for all cases since this would depend on the function and type of structure. But considering the information presented here, cracking of panel walls in frame structures is likely when angular distortion exceeds 1/300, and damage to the structure itself is likely when angular distortion exceeds 1/150. More stringent limits should be established for load-bearing wall structures.

Chapter 4

SUBSIDENCE PREDICTION

4.1 General Remarks

Liquefaction is a very complicated problem. It may not be analytically possible to accurately evaluate the damage as well as the corresponding risk. Moreover, there could be numerous possible damage scenarios in earthquake-induced liquefaction. Some limit (extreme) cases can be studied for this purpose. The upper or lower bound estimate of the probability of damage estimated from the limit cases could be meaningful in many cases. Subsequent refinements should help to narrow the difference between the upper and lower bound probabilities of damage. Even the information on relative risk could be used in a decision analysis framework.

One extremely conservative limit case that is considered in this study is liquefaction as a subsidence problem. This case could be visualized as the collapse of a tunnel in a soft deposit and its consequences. For a liquefaction problem this case can be modeled as a subsidence problem where all the liquefied soil volume has flowed away from beneath the foundation, creating a void. Thus, a basic understanding of the subsidence problem is necessary. A brief review of the subsidence problem is given in the following sections.

4.2 Subsidence

The problem of predicting ground surface movement above a subsurface void or cavity is not new. A considerable amount of research has been conducted on this problem since the beginning of the nineteenth century (49).

Basically, the problem is to calculate a priori the horizontal and vertical displacements of the ground surface in the event that a volume of soil is removed from below the ground surface. This problem is of considerable interest to mining and tunneling engineers, and it is in these two disciplines that the state of the art in subsidence prediction is well developed (6,7,20,46,49,50,60).

By the 1960's, there was general agreement on the mechanism of subsidence (49). A void created in the soil below the surface disturbs the existing stress field. Displacement and deformation are induced in the soil surrounding the void to restore equilibrium. These ground movements could extend to the surface depending on the depth of the void, its dimensions and the character of the soil overlying the void. If the void is sufficiently large, the soil immediately above the void breaks away and falls into the void. The layers of soil above the failure region may remain intact rather than breaking, assuming fairly regular trough-shaped curves as they span the failure region. Subsidence of the soil layers may develop up to the ground surface depending on the bulking characteristics of the soil (49).

In the case of a subsurface void of constant thickness lying in a horizontal plane, the resulting surface subsidence has several distinctive characteristics. Points on the ground surface above the void are displaced both in the vertical and horizontal directions. The vertical displacement or subsidence forms a "subsidence trough" which in plan view extends beyond the bounds of the void, while the horizontal displacements are larger than would be expected from just the curvature of the subsidence trough. In addition, the vertical and horizontal displacement of the ground surface will be symmetrical about the centerline at the subsidence trough, with the

center point being the point of maximum subsidence and of zero horizontal displacement (10).

Several parameters are important in describing subsidence. Fig. 4.1 shows in elevation a soil deposit with a void below the surface and the resulting subsidence of the ground surface. The void is assumed to lie in a horizontal plane and to be of constant thickness, m. L is defined as the half-width of the void, h is the depth of void, s(x) is the vertical displacement or subsidence of the ground surface at a horizontal distance X from the center of the subsidence through, and α is the angle of draw or limit angle, which is defined as the angle measured from the horizontal to the line connecting the edge of the void with the point of zero subsidence on the ground surface.

For each void thickness, m, there is an upper limit to the amount of surface subsidence regardless of the plan dimensions of the void (10,41, 49,50). This maximum subsidence is called full subsidence, S_{max}. The magnitude of S_{max} will depend on the soil and its bulking properties. Whether full subsidence is developed at the surface depends on the width of the void relative to its depth. Accordingly, three levels of subsidence can be identified, namely subcritical, critical and supercritical. If the surface subsidence, s, is smaller than S_{max} everywhere, then the subsidence is subcritical; if s is equal to S_{max} at just one point, then the subsidence is critical; if s is equal to S_{max} in a region of the subsidence trough, then the subsidence is supercritical (Fig. 4.1).

Many methods have been developed to predict ground movements over subsurface voids. Most of these methods can be classified as one of two types, empirical or phenomenological. The more successful methods will be

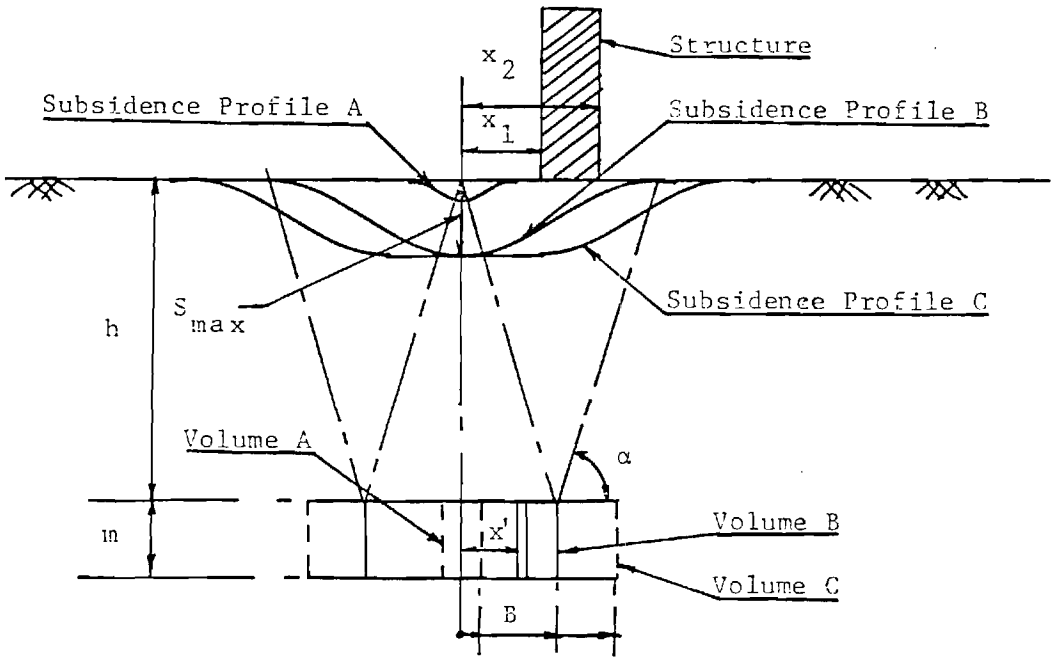

Fig. 4.1 Subsidence Profile

discussed here in the context of predicting ground subsidence over a subsurface horizontal void of constant thickness.

4.3 Empirical Methods

The empirical approaches are based on observations of ground movements without particular regard to the mechanics of subsidence (60). Vertical and horizontal displacement of the ground service are related to the type of subsurface soil, dimensions of the void and depth of the void from the surface through empirical generalizations of field subsidence data.

The fundamentals of the empirical methods can be reduced to two fundamental relationships. The first empirical generalization is that the full subsidence, S_{max}, is related to the void thickness, m, by the following equation:

$$S_{max} = a\ m \tag{4.1}$$

where a is called the subsidence factor. The subsidence factor depends on the type of soil and the depth of the void below the surface, but it is usually considered just as a function of soil type (10,50,62). The second empirical generalization is that for a point P on the surface, the region of a horizontal void which contributes to the subsidence of P (often called the area of influence) is a circle of radius B ; the circle forms the base of a right circular cone with apex at point P (10,49). B is called the critical width and is given by the following equation.

$$B = h \cot \alpha \tag{4.2}$$

where h and α are defined as before. Subcritical, critical and supercritical subsidence can now be defined in terms of the critical width, B. If the half-width of the void, L, is greater than B, then the subsidence is supercritical; if L is equal to B, then the subsidence is critical; and if L is less than B, then the subsidence is subcritical.

The subsidence profile (the subsidence of the ground surface between the points of maximum subsidence and zero subsidence) may be predicted empirically by a number of methods. The more common methods are the method of the National Coal Board (39), the method of profile functions and the method of influence functions (7,10,49,50). These methods are briefly discussed below.

4.3.1 Method of the National Coal Board

The method developed by the National Coal Board of the United Kingdom is perhaps the most comprehensive and widely used empirical method (7). It is based on subsidence data from numerous field surveys in Great Britain (60). The data from the field surveys has been presented in the form of empirical graphs and procedures to facilitate the prediction of subsidence profiles. Regardless of the type of subsurface material, the same subsidence factor, a, and the same subsidence profile are used for subsidence calculations (39).

The advantages of this method are its simplicity and reliability. The accuracy of subsidence calculations is claimed to be $\pm$10% in most cases. Prediction of horizontal displacement is not as accurate (60). The disadvantages are that a considerable amount of field data is required for high statistical confidence, the effect of soil type on the subsidence factor and subsidence profile is not taken into account, the subsurface void must be rectangular in shape with the length much greater than the width, the subsurface material must be relatively homogeneous, and the high uncertainty involved in extrapolating the conditions other than the conditions in the original field surveys.

4.3.2 Method of Profile Functions

The method of profile functions is similar to the method of the National Coal Board except that different subsidence factors are used for different regions and the subsidence profile is assumed to be described by a smooth mathematical function called a profile function. Specifically, the profile function is an equation of one-half the subsidence profile, ranging from full subsidence to zero subsidence (10). These functions are usually determined from field observations. Brauner (10) has given several examples of different profile functions.

Unlike the method of the National Coal Board, the effect of local geology on the shape of the subsidence profile is indirectly taken into account by using different profile functions for different conditions. However, the method is still restricted to voids of rectangular geometry with a long side and homogeneous soil deposits. The method is fairly simple to use but requires a large amount of field data for high statistical confidence.

4.3.3 Method of Influence Functions

In the method of influence functions, the subsurface void is imagined as consisting of an infinite number of infinitesimal void elements. Each infinitesimal void is thought to contribute a small amount to the subsidence at the surface. The complete subsidence profile is the sum of all the small subsidences due to each infinitesimal void element (7,10,50).

It is supposed that the subsidence at the ground surface due to an infinitesimal void element can be represented by an influence function, and that the principle of superposition can be applied so that the total effect of all the infinitesimal elements is additive (7). Brauner (10) has given several examples of different influence functions.

In general, the influence function is represented by $f(r',r)$, where r' is the horizontal distance at the level of the void measured from a vertical axis located at the center of the void and r is the horizontal distance at the level of the ground surface measured from that same vertical (Fig. 4.1). The surface subsidence at the point r is given by the following equation (7,10):

$$s(r) = \iint_A f(r',r)\, da \tag{4.3}$$

where the integral is evaluated over the plan area of the void, A. The advantages of Eq. 4.3 is that surface subsidence may be calculated even for voids of arbitrary shape. In the case of long voids, it is sufficient to evaluate a single integral instead of the double integral in Eq. 4.3.

The most appropriate influence function for a cohesionless soil and a long void can be represented by the following equation (60):

$$f(x',x) = \frac{S_{max}}{B} \cdot \exp\left[-\pi\left(\frac{x' - x}{B}\right)^2\right] ; \; |x' - x| \leq B \tag{4.4}$$
$$= 0 \; ; \text{ elsewhere}$$

where x' is the horizontal distance at the level of the void measured from the center and along the width of the void, and x is the horizontal distance at the level of the ground surface measured from the center and along the width of the subsidence trough (Fig. 4.1).

For a long void the surface subsidence is found by integrating Eq. 4.4 over the width of the void, 2L, i.e.,

$$S(x) = \int_{-L}^{L} f(x',x)\, dx' \tag{4.5}$$

The differential settlement between two points located x_1 and x_2 distances from the origin is thus

$$\delta_{12} = | S(x_1) - S(x_2) | \tag{4.6}$$

The corresponding rotation can be defined as

$$\theta_{12} = \frac{\delta_{12}}{x_2 - x_1} \tag{4.7}$$

The absolute rotation, ρ, at a point of the ground surface can be obtained by calculating the derivative of Eq. 4.5, i.e.,

$$\rho(x) = \left| \frac{d}{dx} \int_{-L}^{L} f(x',x)\, dx' \right| \tag{4.8}$$

Substituting Eq. 4.4 in Eq. 4.7, the maximum value of the slope can be shown to be

$$\rho_{max} = \frac{S_{max}}{B} = \frac{a\ m}{B} \tag{4.9}$$

The critical length parameter B is given by

$$B = h \cot \alpha \tag{4.10}$$

in which α = the limit angle of influence, as shown in Fig.4.1. Terzaghi (55) considered a problem similar to this one in connection with arching action in soils. The angle α may approach 90^o for very small values of h; however, it approaches a value of $45^o + \phi/2$ for large values of h. ϕ is the angle of internal friction for the soil. Typical α and ϕ values are given in Table 4.1.

The subsidence factor a can be estimated as

Table 4.1- ϕ and α Values for Sand Deposits
(from Ref. 62)

Soil Condition	Relative Density	ϕ	α
Very Loose Sand	< 20%	< 29°	< 59.5°
Loose Sand	20 - 40%	29 - 30°	59.5 - 60°
Medium Sand	40 - 60%	30 - 36°	60 - 63°
Dense Sand	60 - 80%	36 - 41°	63 - 65.5°
Very Dense Sand	> 80%	> 41°	> 65.5°

$$a = \left[\frac{3}{2}\ \frac{\gamma_f - \gamma_o}{\gamma_f}\ \cdot\ \frac{h}{m}\right] + 1 \qquad (4.11)$$

in which γ_o and γ_f are the unit weight of soil before and after the subsidence has occurred. Eq. 4.11 yields similar values to those given by Brauner (10). The values of a are expected to be between 0.1 and 0.9 for sand deposits.

It must be pointed out here that the ρ_{max} value obtained by using Eq. 4.9 is the maximum slope of the subsidence curve occurring at a point. In reality, angular distortion, the differential settlement divided by the foundation length, is a better measure of damage. ρ_{max} always over-predicts the level of damage.

A more realistic measure of damage would be the parameter θ_{12} in Eq. 4.7. To obtain the maximum rotation or to maximize θ_{12} under the constraint that $x_2 - x_1 = d = \text{constant}$, the method of Lagrange Multipliers can be used. Following the method of Lagrange Multipliers, the set of equations that must be solved are:

$$\underset{\sim}{\nabla}\ \theta_{21} = \left(\frac{\partial \theta_{21}}{\partial x_1}\ ,\ \frac{\partial \theta_{21}}{\partial x_2}\right) = \lambda\ \underset{\sim}{\nabla}\ q \qquad (4.12)$$

and $g(x_1, x_2) = x_2 - x_1 - d = 0$

in which $\underset{\sim}{\nabla}$ is the gradient and λ is the Lagrange multiplier. Solving Eq. 4.12, it can be shown that x_1 and x_2 are located at a distance d/2 from the inflection point of the subsidence profile. The maximum value of θ_{12} can be shown to be

$$(\theta_{12})_{max} = \frac{S_{max}}{d}\left[2\ \Phi\left(\frac{d\ 2\pi}{2B}\right) - 1\right] \qquad (4.13)$$

This will be discussed further in Chapter 5.

Influence functions analogous to the vertical displacement influence functions just discussed can be derived for the purposes of calculating horizontal displacement of points on the ground surface. With this information and Eq. 4.5, horizontal and vertical strain, rotation and curvature of the ground surface can be calculated. This will be evaluated in detail in subsequent studies.

The method of influence functions and the method of profile functions differ only in the way they describe the subsidence profile. The method of profile functions describes the subsidence profile with a single function; the method of influence functions describes the subsidence profile with an integral form (Eq. 4.5). A disadvantage of influence functions is that they cannot be measured directly from the field data as profile functions can. In addition, to find the subsidence profile, the principle of superposition must hold. The main advantages of the method, however, are its simplicity, its ability to account for, if only indirectly, the effects of local geology and its ability to treat voids of arbitrary shape.

4.4 Phenomenological Methods

Whereas the empirical methods were based on field measurements of actual ground subsidence, phenomenological methods are based on laboratory or field measurements of material properties (10). Displacement and strain of the soil surrounding the subsurface voids are derived from the principles of continuum mechanics. The behavior of the subsurface material is accounted for through the stress-strain laws, i.e. constitutive laws. In most cases these constitutive laws are mathematical idealizations of the real material behavior.

The more common phenomenological approaches are soil mechanics methods, the classical elasticity models, the viscoelastic models, the

post-yield models, and the finite element method. For the most part, these methods differ depending on how they treat the material behavior, the boundary conditions, anisotropy and nonhomogeneity.

4.4.1 Methods of Soil Mechanics

Terzaghi (55), in conjunction with his study on arching behavior in soils, was the first to consider the subsidence problem from a soil mechanics perspective. He was principally concerned with describing the slip surfaces in the soil surrounding the subsurface void. Obert (41) detailed how the Coulomb-Mohr yield criterion together with Mohr's circle could be used to calculate the orientation of the failure surfaces. Post-yield behavior was not discussed in either study. Thus, from these studies, the surface subsidence cannot be found.

4.4.2 Classical Elasticity Models

In these methods the subsurface material is treated as elastic. The displacement and stresses in the elastic medium surrounding a thin rectangular void are found by solving the displacement discontinuity model (7,57). Solutions for the two-dimensional, homogeneous, isotropic and transversely isotropic cases are given in the literature as well as a treatment of the three-dimensional case (7,57). The effect of incomplete closure of the void on the surface displacement has also been studied (8). Results of the transversely isotropic case agreed reasonably well with field observations (60).

The merit of the classic elasticity approach is that it attempts to model the underlying mechanics of subsidence even though the elastic assumption may not be entirely justified. A region of material below the surface may behave elastically, but the material immediately surrounding the void is in a state of yield. The main drawbacks of the method are that

the boundary conditions and the in situ values of the material parameters needed for the analysis are very difficult to determine. Furthermore, the method is not well suited to treat nonhomogeneous conditions.

4.4.3 Viscoelastic Models

Viscoelastic models were developed in order to incorporate time dependence into subsidence models. In these approaches the subsurface material is treated as a linearly viscoelastic medium. Berry (7) and Imam (33) have reported solutions to this problem. Close agreement with field observations was obtained (60).

This method suffers from the same difficulties as the classical elasticity models. In addition, there is some experimental evidence to suggest that viscoelastic analysis may be inappropriate (7,60).

4.4.4 Post-Yield Solutions

Attempts have been made to incorporate the post-yield behavior of the failure zone surrounding the void into the subsidence analysis. Most of this work has been with physical simulation (19,53,60). Results of these model studies are expected to shed light on the subsidence mechanism. However, post-yield methods will suffer from the same difficulty as the other phenomenological approaches, and that is determining the in situ values of the material parameters.

4.4.5 Finite Element Methods

Even if the material models of the other phenomenological methods correctly describe the behavior of the subsurface material, strong non-homogeneity of the material properties throughout the deposit may invalidate the results from these methods. Finite element methods are well suited to account for nonhomogeneity. In addition, situations with an irregular ground surface or a void of arbitrary shape can be analyzed with

this method (7,63). The disadvantage of this method is that the number of equations to be solved increases with the number of elements. For a typical subsidence analysis, the region to be analyzed extends for a considerable distance below and to each side of the void, requiring a considerable number of elements for an adequate analysis and a considerable amount of computational effort. In addition, the material parameters need to be specified.

4.5 Mechanics of Stochastic Media

There is some doubt as to whether sufficiently reliable results for surface subsidence can be obtained by representing a granular material like a cohesionless soil by a continuum. In contrast to the continuum description, the mechanics of stochastic media treats the subsurface material as a discontinuous medium. Specifically, the soil deposit is represented as a layered sequence of small cubical cells where each cell contains a ball which represents a soil particle (Fig. 4.2). Subsidence over a subsurface void can be simulated by removing a ball from a lower cell. This cell is replaced, with equal probability, by a ball from one of the two cells immediately above. In this way a void will propagate from the lower level to the surface. If a large number of balls are removed from the lower cells a subsidence trough will be formed at the surface. Sweet and Bogdanoff (54) have shown that for small voids the average subsidence profile of the surface will approach the characteristic bell shape of the normal distribution function. This conclusion is also supported by the results of model studies performed by Sweet (53).

Litwiniszyn (38) conceived the phrase "mechanics of stochastic media" to describe his mathematical theory of ground subsidence. However, there is nothing stochastic about it. The differential equations that are

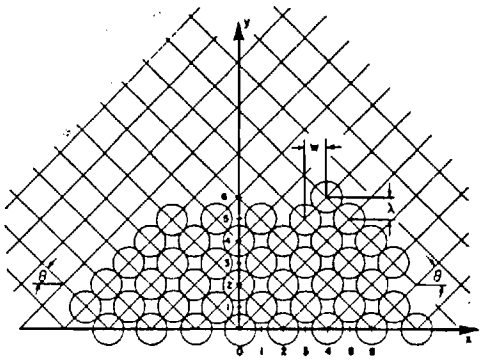

Fig. 4.2 Stochastic Model for Soil Medium (54)

developed to describe ground subsidence resemble the Fokker-Planck equations in the theory of stochastic processes; hence, the phrase "stochastic media". Though the mathematical formulation is very appealing, some of the assumptions regarding the kinetics of subsidence are not warranted.

4.6 Conclusions

The more common methods available to estimate the subsidence of the ground surface over a subsurface void have been discussed. Most of the methods can be classified broadly as either an empirical or a phenomenological approach. The empirical approaches are characterized by simplicity, while the phenomenological methods are extremely complicated. The main practical difference between the two types of methods is that the phenomenological models are based on laboratory and field measurements of material properties while empirical methods are based on field measurements of actual ground movements (10). Since the phenomenological methods are still in the development stage and the empirical methods have gained wide acceptance in the profession (10), an empirical approach, the method of influence functions, is used in this study.

Chapter 5

LIQUEFACTION-INDUCED DAMAGE

5.1 General Remarks

A three-dimensional probabilistic liquefaction model, damage criteria, and a very simplified model to estimate damage were developed in the previous three chapters. The stage is now set to put them together to estimate damage in earthquake-induced liquefaction. As discussed in Chapter 4, angular deformation ρ (Eq. 4.8) or θ (Eq. 4.7) will be used here as an indicator of damage. To estimate the risk associated with a particular angular deformation, the following concept is used.

The amount of rotation of foundation due to liquefaction depends on the liquefied volume, deposit conditions, depth of the volume from the ground surface, etc. Thus, the amount of rotation can be related to the soil volume. For the same soil volume, the risk of liquefaction can also be estimated as discussed in Chapter 2. Thus, for the same volume, it is possible to estimate the risk associated with different amounts of rotation due to earthquake-induced liquefaction. This concept can be explained effectively with the help of an example.

5.2 Example

A site in Niigata, Japan which liquefied during the 1964 earthquake is considered here. The magnitude of the earthquake was 7.5 and the site experienced 0.16 g maximum ground acceleration. The SPT value of 6 was measured at the critical depth of 25 ft. The depth of the water table was 3 ft. from the ground surface. The saturated unit weight and the mean grain size, D_{50}, were considered to be 120 pcf and 0.26 mm, respectively. The maximum and minimum dry densities of the deposit are considered to be

102.7 pcf and 81.5 pcf, respectively, from indirect information. The scales of fluctuation, θ_x, θ_y, and θ_z can not be estimated for the site. The scales of fluctuation in the two horizontal directions are assumed to be the same. θ_x, θ_y, and θ_z are considered to be 120 ft., 120 ft., and 7 ft., respectively. The volume of the liquefied sand is assumed to be 200 ft. x 200 ft. x 5 ft. The COV of γ_s and h_{WT} can be taken as 0.01 and 0.20, respectively. Using Equation 2.13, Haldar and Miller showed that the risk of liquefaction of the soil volume would be around 0.98.

To show the application of the general three-dimensional probabilistic liquefaction model, the aforementioned site conditions can be assumed to exist in deposits in the San Francisco Bay area and in San Juan, Puerto Rico. These sites are considered here since the seismic risk of the areas is available in the literature. In Fig. 5.1, the annual risks of liquefaction using Eq. 2.14 versus the Standard Penetration Test (SPT) values are plotted for various soil volumes. As expected, some difference is noticeable. When a site is designed against liquefaction, the annual risk of liquefaction would be much smaller. In that case, the differences between different volumes of sand would be considerable. This is also shown in Figure 5.1.

To estimate the damage associated with the earthquake-induced liquefaction, SITE A in Fig. 5.1 is considered here. A soil volume of 100' x 100' x m is considered for this illustrative example. The angle of internal friction ϕ is assumed to be 36^o. For a = 0.1, 0.2, and 0.6 (Eq. 4.1), the amount of rotation ρ_{max} (Eq. 4.9) as well as the risk of liquefaction is calculated for SPT values of 6 and 15. The risk versus rotation is plotted in Fig. 5.2. It must be pointed out here that the ρ_{max} values in Fig. 5.2 are upper bound estimates of rotation. The total

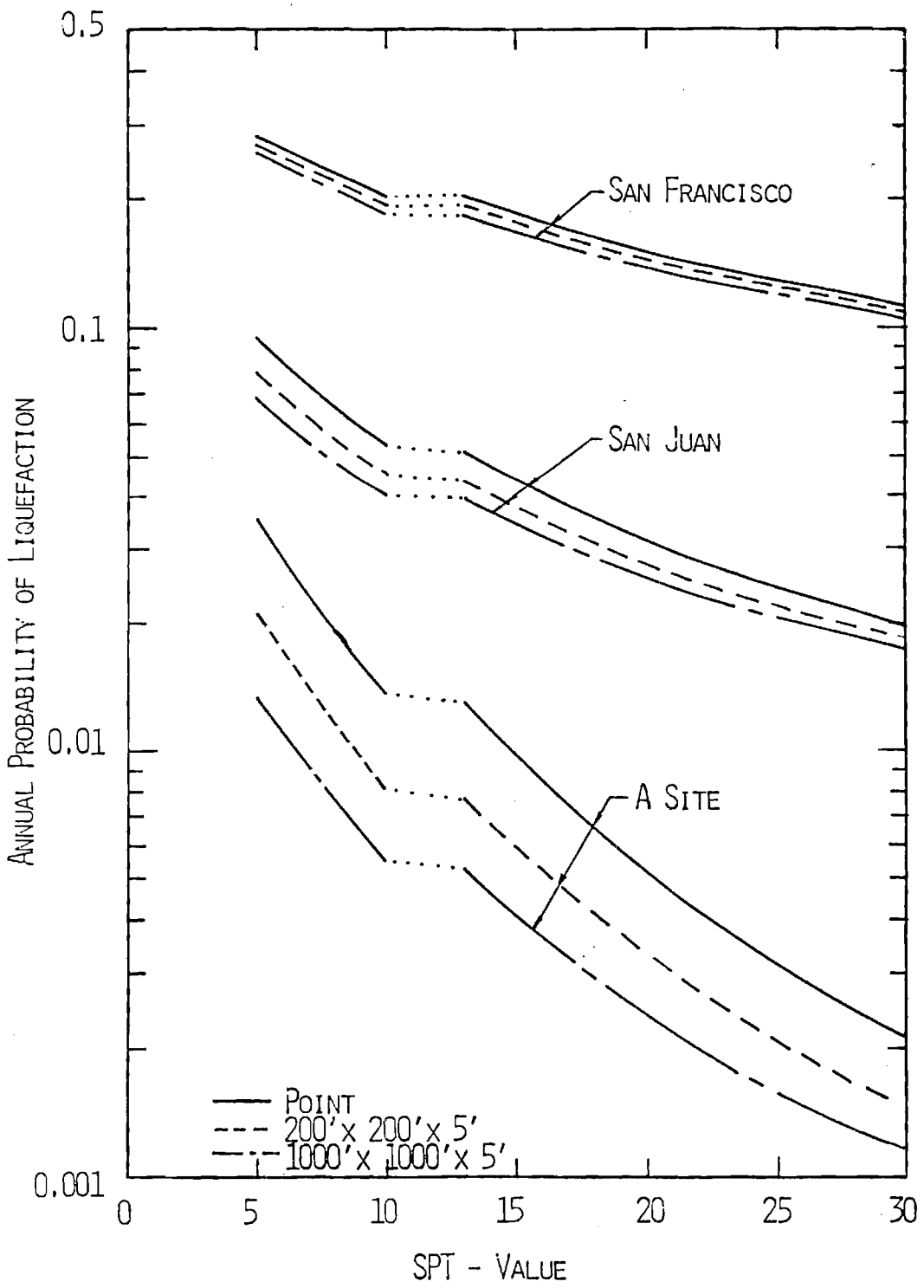

Fig. 5.1 Estimated Annual Probability of Liquefaction

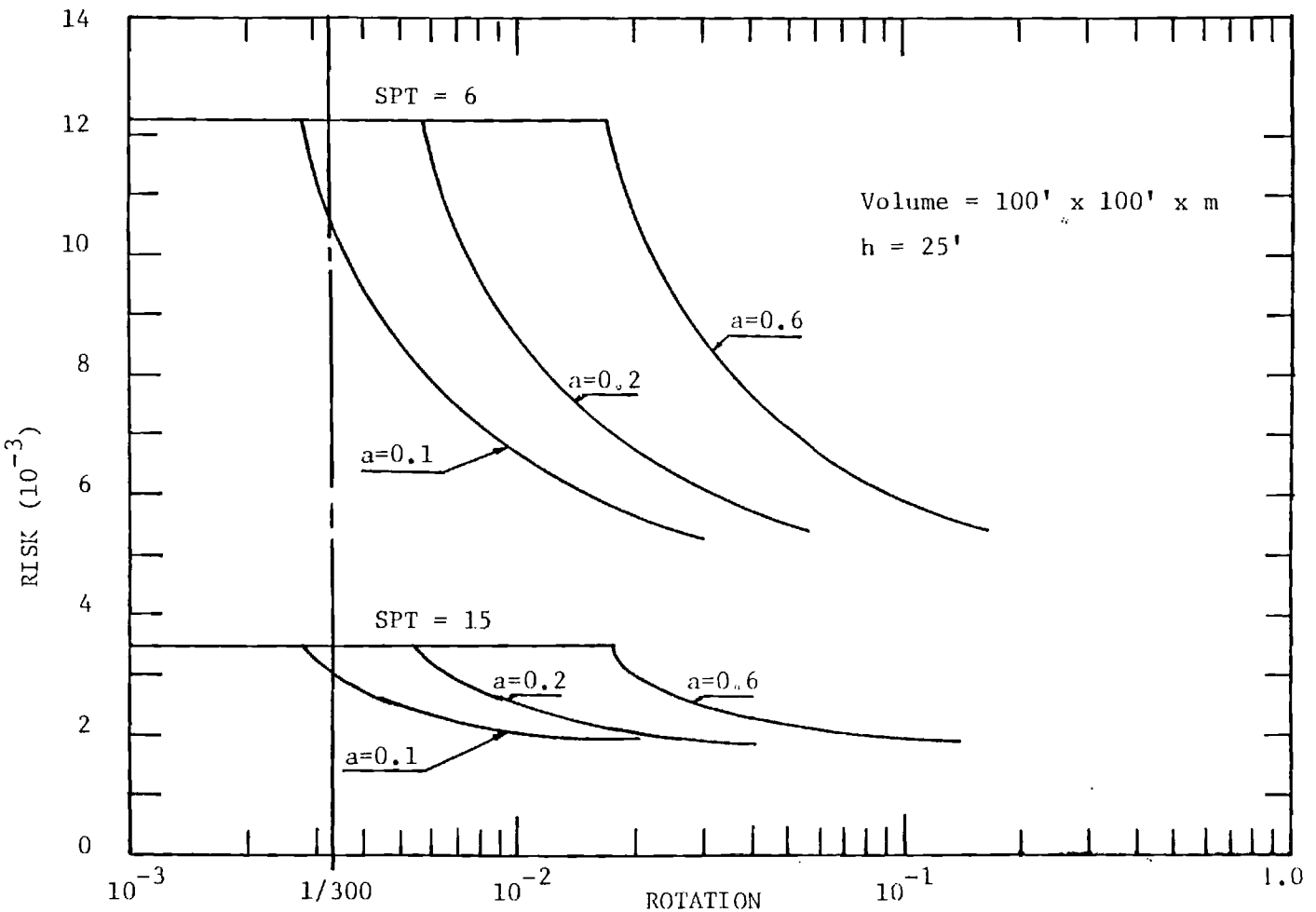

Fig. 5.2 Risk of Earthquake-Induced Rotation

liquefied volume is not expected to flow away beneath the foundation creating a void. Thus, the a values that need to be considered to estimate ρ_{max} would be much smaller than in the pure subsidence problem. In addition, ρ_{max} is the maximum slope of the subsidence curve occurring at a point. In reality, angular distortion, the differential settlement divided by the foundation length, is a better measure of damage. Thus, ρ_{max} always overpredicts the level of damage. Angular rotation (Eq. 4.7) will be discussed in the following paragraphs.

Some interesting observations can be made from Fig. 5.2. The risk of rotation depends on the SPT values and the subsidence factor. As the site becomes denser, the risk of a given amount of rotation decreases. Also, the subsidence factor contributes significantly to the estimation of rotation. A lower value of a is expected due to earthquake-induced liquefaction. The most appropriate value of a needs to be calibrated using case studies. This work is now in progress. It can also be observed from Fig. 5.2 that the risk decreases as the value of the tolerable rotation increases. The tolerable rotation for ordinary buildings, generally accepted by the profession is 1/300 (Section 3.6). For the problem under consideration, the risks of 1/300 rotation for SPT values of 6 and 15 are 1.2×10^{-2} and 3.5×10^{-3}, respectively. The corresponding annual risks of liquefaction are found to be 2.2×10^{-2} and 8×10^{-3}, respectively. These higher risks are expected. They clearly indicate that the risk of liquefaction and risk of damage are different and need to be considered separately. It is also interesting to note that as the value of acceptable rotation increases, the corresponding risk decreases significantly.

As discussed earlier, the ρ_{max} value shown in Fig. 5.2 may not be a true indicator of damage. The more appropriate parameter would be θ (Eq.

4.7). Thus, it is necessary to correlate the ρ_{max} and θ values. For the site under consideration, some typical results are given in Table 5.1. It can be observed from Table 5.1 that the ρ_{max} and θ values are similar only when the length of the structure, d, is small. However, for any real structure the θ values are considerably smaller than the ρ_{max} values. Efforts are now being made to develop figures similar to Fig. 5.2 for θ versus the annual risk. This would give a more realistic measure of damage.

Table 5.1 - ρ_{max} and θ values for a = 0.1

and for SITE A

ρ^*_{max} ($\times 10^{-3}$)	d (ft) / m (ft)	θ^* ($\times 10^{-3}$)					
		1	5	10	25'	50'	100'
0.785	0.1	0.784	0.755	0.675	0.394	0.200	0.100
3.925	0.5	3.919	3.773	3.374	1.972	1.000	0.500
7.851	1.0	7.838	7.545	6.748	3.944	2.000	1.000
15.701	2.0	15.675	15.090	13.497	7.889	4.000	2.000
39.253	5.0	39.828	37.587	33.650	19.722	10.000	5.000
78.51	10.0	79.656	75.173	67.300	39.444	20.000	10.000

*Multiply ρ_{max} and Θ values by 2.0 when a = 0.2, and by 6.0 when a = 0.6

Chapter 6

SUMMARY AND CONCLUSION

6.1 Summary

A three-dimensional probabilistic liquefaction model is developed here to estimate the risk of damage due to earthquake-induced liquefaction. The uncertainties associated with the load and resistance parameters are considered in this model. The load model considers the uncertainty in the seismic loading. The resistance model includes the uncertainty associated with the laboratory estimation as well as the field estimation of a geotechnical parameter. Detailed uncertainty analysis of each parameter is not done in this report for the sake of brevity; however, they are discussed in detail elsewhere (28).

The scale of fluctuation of a parameter representing the site conditions is important input information for the model. Several methods available to calculate the scale of fluctuation are discussed. Some practical alternatives for geotechnical applications are proposed.

A detailed discussion is made to quantify damage associated with earthquake-induced liquefaction. The damage is expressed in terms of absolute settlement, differential settlement, and rotation. To estimate the allowable values of these parameters, all major codes, standards, and guidelines are reviewed and compared in this study. The deficiencies and non-uniformities in these guidelines are also outlined. Some recommendations are made regarding the allowable values of damage parameters.

There could be numerous possible damage scenarios in earthquake-induced liquefaction. One extremely conservative limit case that is considered in this study is liquefaction as a subsidence problem. For a

liquefaction problem this case can be modeled as a subsidence problem where all the liquefied soil volume has flowed away from beneath the foundation, creating a void. To understand the subsidence problem, all available empirical, phenomenological and stochastic media approaches are reviewed and documented. Using these models, expressions are derived to estimate the maximum settlement, differential settlement, slope, and rotation.

All this information is used to develop a probabilistic model to evaluate the risk associated with earthquake-induced liquefaction. This model will be developed further in the subsequent study.

6.2 Conclusions

On the basis of the results obtained from this study, the following major conclusions can be reached:

(i) The risk of liquefaction at a site needs to be estimated considering the damage aspect of the problem. It is necessary to consider the minimum soil volume that will produce a noticeable amount of damage at the referenced point when it liquefies. Soil properties in that soil volume need to be modeled probabilistically in three dimensions.

(ii) The model uses the information on the scale of fluctuation of a parameter to represent its three-dimensional characteristics. Several methods are available to estimate the scale of fluctuation, as discussed in this report. Some practical approaches are also suggested for geotechnical use.

(iii) Damage is a very controversial term. However, it can be evaluated in terms of absolute settlement, differential settlement, slope or rotation of a foundation. Allowable values for these parameters are not

available in a usable form in major design codes, standards, and guidelines. When available, they vary widely. These guidelines need to be made uniform.

(iv) The liquefaction problem can be modeled as a subsidence problem. Obviously, this is a very conservative limit case. This model needs to be refined in the future, and this will be done in a subsequent study. The results obtained from the present simplified model are quite informative in terms of annual risk versus the settlement or rotation. The major contribution of this model is that it considers all the important parameters that can be associated with the damage caused by earthquake-induced liquefaction.

(v) The proposed probabilistic model provides information on the relative risk of damage associated with earthquake-induced liquefaction for various design alternatives. This information will be valuable to designers in selecting the appropriate design alternatives.

LIST OF REFERENCES

1. American Institute of Steel Construction, Inc., Manual of Steel Construction, 8th ed., Chicago, Ill., 1980.

2. American Concrete Institute, ACI Standard 318-77, Building Code Requirements for Reinforced Concrete, Detroit, Mich., 1977.

3. American Association of State Highway and Transportation Officials, Standard Specification for Highway Bridges, Twelfth ed., Wash., D.C., 1977.

4. American National Standards Institute, ANSI A58.1-1982, American National Standard: Minimum Design Loads for Buildings and Other Structures, N.Y., 1982.

5. Applied Technology Council, National Bureau of Standards, ATC 3-06, NBS SP-510, NSF 78-8, Tentative Provisions for the Development of Seismic Regulations for Buildings, June 1978.

6. Attewell, P., "Ground Movements Caused by Tunneling in Soil, Proceedings on Large Ground Movements and Structures, Cardiff, July, 1977, pp. 812-948.

7. Berry, D.S., "Progress in the Analysis of Ground Movements Due to Mining," Proceedings on Large Ground Movements and Structures, Cardiff, July, 1977, pp. 781-811.

8. Berry, D.S. and Sales, T., "Elastic Treatment of Ground Movement Due to Mining," Journal of Mechanics and Physics of Solids, Part 2, Vol. 9, No. 1, Feb., 1961, pp. 52-62; Part 3, Vol. 10, No. 5, Jan., 1962, pp. 73-83.

9. Bjerrum, L., "Allowable Settlement of Structures," Proceedings of the European Conference on Soil Mechanics and Foundation Engineering, Weisbaden, Germany, 1963, Vol. III, pp. 135-137.

10. Brauner, G., "Subsidence Due to Underground Mining," Information Circular 8571, United States Department of the Interior, 1973.

11. Burland, J.B., and Wroth, C.P., "Allowable and Differential Settlement of Structures, Including Damage and Soil-Structure Interaction," Proceedings, Conference on Settlement of Structures, Cambridge University, Cambridge, England, 1974, pp. 611-654.

12. Christian, J.T. and Swiger, W.F., "Statistics of Liquefaction and SPT Results," Journal of the Geotechnical Engineering Division, ASCE, Vol. 101, No. GT11, Proc. Paper 11701, Nov. 1975, pp. 1135-1150.

13. Cornell, C.A., "Engineering Seismic Risk Analysis," Bulletin of Seismological Society of America, Vol. 58, No. 5, Oct. 1968, pp. 1583-1606.

14. DeAlba, P., Chan, C.K. and Seed, H.B., "Determination of Soil Liquefaction Characteristics by Large-Scale Laboratory Tests, Earthquake Engineering Research Center Report No. EERC 75-14, University of California, Berkeley, May 1975.

15. Derkiureghian, A. and Ang, A. H-S., "Fault-Rupture Model for Seismic Risk Analysis," Bulletin of Seismological Society of America, Vol. 67, No. 4, Aug. 1977, pp. 1173-1194.

16. Donovan, N.C., "A Stochastic Approach to the Seismic Liquefaction Problem," Proceedings, Conference on Statistics and Probability in Soil and Structural Engineering, Hong Kong, Sept. 1971, pp. 513-535.

17. Faccioli, E., "A Stochastic Model for Predicting Seismic Failure in a Soil Deposit," Earthquake Engineering and Structural Dynamics, Vol. 1, 1973, pp. 293-307.

18. Fardis, M.N., and Veneziano, D., "Probabilistic Liquefaction of Sands During Earthquakes," Report No. R79-14, Massachusetts Institute of Technology, Cambridge, Mass., March 1979.

19. Farmer, I.W. and Altounyan, P.F.R., "The Mechanics of Ground Deformation Above a Caving Longwall Face," Proceedings of Ground Movements and Structures, Cardiff, April 1980, pp. 75-91.

20. Ghaboussi, J., Ranken, R.E., and Karshenas, M., "Analysis of Subsidence Over Soft-Ground Tunnels," Proceedings, Evaluation and Prediction of Subsidence, Edited by S.K. Saxena, January 1978.

21. Grant, R., Christian, J.T., and Vanmarcke, E.H., "Differential Settlement of Buildings," Journal of the Geotechnical Engineering Division, ASCE, Vol. 100, No. GT9, Proc. Paper 10802, Sept. 1974, pp. 973-991.

22. Haldar, A., "Liquefaction Study - A Decision Analysis Framework," Journal of the Geotechnical Engineering Division, ASCE, Vol. 106, No. GT12, Proc. Paper 15925, pp. 1297-1312, December 1980.

23. Haldar, A., Chapter 6 - Statistical Methods, Numerical Methods in Geomechanics, edited by J.B. Martins, NATO Advanced Study Institute Series, D. Reidel Publishing Company, Boston, 1981.

24. Haldar, A., "Probability of Liquefaction in a 3-D Soil Deposit," Invited Presentation, Proceedings, Applications of Probabilistic Methods in Geotechnical Engineering, U.S. Army Waterways Experiment Station, Vicksburg, Mississippi, September 1982.

25. Haldar, A., "Risk of Damage in Liquefaction," Specialty Conference on Probabilistic Mechanics and Structural Reliability, Berkeley, California, January 11-13, 1984.

26. Haldar, A., "Statistical Site Characterization," Fourth Australia-New Zealand Conference on Geomechanics, Perth, Australia, May 14-19, 1984.

27. Haldar, A., and Miller, F.J., "Probabilistic Evaluation of Liquefaction in a 3-D Soil Deposit," International Conference on Soil Dynamics and Earthquake Engineering, Southampton, U.K., July 1982.

28. Haldar, A., and Miller, F.J., "Research Initiation - Probabilistic Evaluation of Damage Potential in Earthquake-Induced Liquefaction in a 3-D Soil Deposit," Report No. SCEGIT-101-82, School of Civil Engineering, Georgia Institute of Technology, Atlanta, March 1982, 134 pages.

29. Haldar, A., and Miller, F.J., "Damage in Liquefaction - Probabilistic Model," Fourth Canadian Conference on Earthquake Engineering, Vancouver, B.C., Canada, pp. 332-340, June 1983.

30. Haldar, A., and Tang, W.H., "Probabilistic Evaluation of Liquefaction Potential," Journal of the Geotechnical Engineering Division, ASCE, Vol. 105, No. GT2, Proc. Paper 14374, Feb. 1979, pp. 145-163.

31. Haldar, A., and Tang, W.H., "Uncertainty Analysis of Relative Density," Journal of the Geotechnical Engineering Divsion, ASCE, Vol. 105, No. GT7, Proc. Paper 14665, July 1979, pp. 899-904.

32. Haldar, A., and Tang, W.H., "Statistical Study of Uniform Cycles in Earthquake Motions," Journal of the Geotechnical Engineering Division, ASCE, Vol. 107, No. GT5, Proc. Paper 16239, pp. 577-589, May 1981.

33. Imam, H.I., "A Viscoelastic Analysis of Mine Subsidence in Horizontal Laminated Strata," thesis presented to the University of Minnesota, at Minneapolis, Minn., in 1965, in partial fulfillment of the requirements for the degree of Doctor of Philosophy.

34. International Conference of Building Officials, Uniform Building Code, 1982 ed., Whittier, California, 1982.

35. Lee, K.L., and Fitton, J.A., "Factors Affecting the Cyclic Loading Strengths of Soil," Vibration Effects of Earthquakes on Soils and Foundation, STP 450, American Society for Testing and Materials, 1969, pp. 71-95.

36. Lee, K.L., and Chan, K., "Number of Equivalent Significant Cycles in Strong Motion Earthquakes," Proceedings, International Conference on Microzonation, Seattle, Washington, Nov. 1972.

37. Leonards, G.A., discussion of "Differential Settlement of Buildings," by Grant, R., Christian, J.T., and Vanmarcke, E.H., Journal of the Geotechnical Engineering Division, ASCE, Vol. 101, No. GT7, July, 1975, pp. 700-702.

38. Litwiniszyn, J., "Application of the Equation of Stochastic Processes to Spatial Problems of Mechanics of Some Types of Bodies," Bulletin De L'Academie Polonaise Des Sciences, Vol. IV, No. 2, 1956, pp. 91-95.

39. National Coal Board, Subsidence Engineer's Handbook, London, U.K., 1975.

40. Naval Facilities Engineering Command, Department of the U.S. Navy, NAVFAC DM-7.1, Design Manual 7.1, Soil Mechanics, Alexandria, Va., May 1982.

41. Obert, L., and Duval, W.I. Rock Mechanics and the Design of Structures in Rock, John Wiley and Sons, New York, N.Y., 1967.

42. Ohsaki, Y., "The Effects of Local Soil Conditions Upon Earthquake Damage," Proceedings, Seventh International Conference on Soil Mechanics and Foundation Engineering, Mexico City, Mexico, 1969.

43. Ohsaki, Y., "Effects of Sand Compaction on Liquefaction During the Tokachioki Earthquake," Soils and Foundations, Vol. 10, No. 2, June 1970, pp. 112-128.

44. Peck, R.B., Hanson, W.E., and Thorburn, T.H., Foundation Engineering John Wiley and Sons, New York, N.Y., 1963.

45. Polshin, D.E., and Tokar, R.A., "Maximum Allowable Nonuniform Settlement of Structures," Proceedings of the 4th International Conference on Soil Mechanics and Foundation Engineering, Vol. 1, London, 1957, pp. 402-406.

46. Scott, R.F., "Subsidence - A Review," Proceedings, Evaluation and Prediction of Subsidence, Edited by S.K. Saxena, January 1978.

47. Seed, H.B., "Soil Liquefaction and Cyclic Mobility Evaluation for Level Ground During Earthquakes," Journal of the Geotechnical Engineering Division, ASCE, Vol. 105, No. GT2, Proc. Paper 14380, Feb. 1979, pp. 201-255.

48. Seed, H.B., and Idriss, I.M., "Simplified Procedure for Evaluating Soil Liquefaction Potential," Journal of the Soil Mechanics and Foundations Division, ASCE, Vol. 97, No. SM9, Proc. Paper 8371, Sept. 1971, pp. 1249-1273.

49. Shadbolt, C.H., "Mining Subsidence," Proceedings on Large Ground Movements and Structures, Cardiff, July, 1977, pp. 705-748.

50. Singh, M.M., "Experience with Subsidence Due to Mining," Int'l. Conf. on Evaluation and Prediction of Subsidence," Pensacola, Fla., Jan., 1978, pp. 92-112.

51. Skempton, A.W. and MacDonald, D.H., "The Allowable Settlements of Buildings," Proceedings of the Institute of Civil Engineers, Vol. 5, Part III, 1956, pp. 727-768.

52. Sowers, G.F., Introductory Soil Mechanics and Foundations: Geotechnical Engineering, Macmillian Publishing Co., Inc., New York, N.Y., 1979.

53. Sweet, A.L., "Validity of Stochastic Model for Predicting Subsidences," Journal of the Engineering Mechanics Division, ASCE, Vol. 91, EM6, Dec., 1965, pp. 111-128.

54. Sweet, A.L., and Bogdanoff, J.L., "Stochastic Model for Predicting Subsidence," Journal of the Engineering Mechanics Division, ASCE, Vol. 91, No. EM2, Proc. Paper 4292, February 1965, pp. 21-45.

55. Terzaghi, K., Theoretical Soil Mechanics, John Wiley and Sons, New York, N.Y., 1943.

56. Terzaghi, K., and Peck, R.B., Soil Mechanics in Engineering Practice, John Wiley and Sons, New York, N.Y., 1948.

57. Tsur-Lavie, Y. and Denekamp, S., "A Boundary Element Method for the Analysis of Subsidence Associated with Longwall Mining," Proceedings on Ground Movements and Structures, Cardiff, April, 1980, pp. 65-74.

58. Vanmarcke, E.H., "Probabilistic Modeling of Soil Profiles," Journal of the Geotechnical Engineering Division, ASCE, Vol. 103, No. GT11, Proc. Paper 13364, Nov. 1977, pp. 1227-1246.

59. Vanmarcke, E.H., Random Fields Analysis and Synthesis, Cambridge, Massachusetts, The MIT Press, 1983.

60. Voight, B., and Pariseau, W., "State of Predictive Art in Subsidence Engineering," Journal of the Soil Mechanics and Foundations Division, ASCE, Vol. 96, No. SM2, Proc. Paper 7187, March 1970.

61. Wahls, H.E., "Tolerable Settlement of Buildings," Journal of the Geotechnical Engineering Division, ASCE, Vol. 107, No. GT11, Proc. Paper 16628, November, 1981, pp. 1489-1504.

62. Winterkorn, H.F., and Fang, H.-Y., "Soil Technology and Engineering Properties of Soils," Foundation Engineering Handbook, Van Nostrand Reinhold Co., N.Y., 1975, pp. 67-120.

63. Wang, M.C., and Baus, R.L., "Settlement Behavior of a Footing Above a Void," Proceedings on Ground Movements and Structures, Cardiff, April 1980, pp. 168-184.

64. Yegian, M.K., and Vitelli, B.M., "Probabilistic Analysis for Liquefaction," Report No. CE-81-1, Department of Civil Engineering, Northeastern University, Boston, Mass., March 1981.

65. Youd, T.L., and Bennett, M.J., "Liquefaction Sites, Imperial Valley, California," Journal of the Geotechnical Engineering Division, ASCE, Vol. 109, No. 3, Proc. Paper 17786, March 1983, pp. 440-457.